Renewable and Sustainable Energy Reviews 220 (2025) 115850

Contents lists available at ScienceDirect

Renewable and Sustainable Energy Reviews

journal homepage: www.elsevier.com/locate/rser

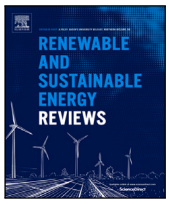

Review article

Parametric resonance in wave energy converters and offshore wind turbines: A review

Josh Davidson [a,b,*], João C.C. Henriques [c], Roberto Galeazzi [d], Tamás Kalmár-Nagy [b]

[a] Basque Center for Applied Mathematics, Mazarredo 14, 48009 Bilbao, Spain
[b] Department of Fluid Mechanics, Faculty of Mechanical Engineering, Budapest University of Technology and Economics, Műegyetem rkp. 3., Budapest, 1111, Hungary
[c] IDMEC, Instituto Superior Técnico, Universidade de Lisboa, Av. Rovisco Pais, 1049-001 Lisboa, Portugal
[d] Department of Electrical Engineering, Technical University of Denmark, DK 2800, Kongens Lyngby, Denmark

ARTICLE INFO

Keywords:
Parametric resonance
Parametric excitation
Dynamic instability
Nonlinear dynamics
Marine renewable energy
Offshore renewable energy
Wave energy
Offshore wind
Floating wind turbine
Spar
TLP
Moorings

ABSTRACT

This review considers the dynamic phenomenon of parametric resonance within marine renewable energy. It consolidates literature on the observation, suppression, exploitation, and modeling of parametric resonance in wave energy conversion and offshore wind turbines. Insights from other offshore industries are integrated, highlighting valuable tools and methods from broader offshore engineering research on parametric resonance. Key gaps are identified, including the need for studies under irregular wave conditions and the impact of parametric resonance on reliability and fatigue life. The review highlights the importance of comprehensive models that integrate hydrodynamic, aerodynamic, and mooring dynamics, coupled with uncertainty analyses, to predict and mitigate parametric resonance's effects across the marine renewable energy device's life cycle.

Contents

* Corresponding author at: Department of Fluid Mechanics, Faculty of Mechanical Engineering, Budapest University of Technology and Economics, Műegyetem rkp. 3., Budapest, 1111, Hungary.
E-mail addresses: josh.davidson@gpk.bme.hu (J. Davidson), joaochenriques@tecnico.ulisboa.pt (J.C.C. Henriques), roga@dtu.dk (R. Galeazzi), kalmar.nagy.tamas@gpk.bme.hu (T. Kalmár-Nagy).

https://doi.org/10.1016/j.rser.2025.115850
Received 12 June 2024; Received in revised form 8 May 2025; Accepted 12 May 2025
Available online 31 May 2025

1. Introduction

Parametric resonance (PR) is a dynamic instability occurring when a system parameter varies periodically. PR can manifest in marine renewable energy (MRE) devices, such as wave energy converters (WECs) and offshore wind turbines (OWTs), due to periodic nature of the marine environment (such as waves) influencing the parameter values of the MRE systems. This instability triggers exponential growth in system oscillations, significantly affecting MRE device performance and safety. The design and optimization of MRE systems depend on understanding component responses to oceanic inputs and effectively managing resonances to achieve optimal techno-economic outcomes. Although the MRE sector is familiar with resonance, the phenomenon of PR has not been explored as extensively. Consequently, a deeper understanding, accurate simulation, and effective PR management are essential for developing cost-effective and reliable MRE solutions.

The effect of PR in ocean engineering is large-amplitude, unstable motions, generally occurring unexpectedly when certain frequency and amplitude conditions are met within a floating structure. In other offshore industries, PR has been studied extensively due to its potential to jeopardize the safety of vessels and floating structures. The nascent MRE industry could benefit from the insights and methodologies developed in these other fields. The present review aims to bridge this knowledge gap by consolidating PR research in MRE, integrating findings from other offshore sectors, and identifying areas where further research is needed. The paper is structured as follows:

- Section 2 is an overview of PR, detailing the theory behind its occurrence in floating bodies.
- Sections 3 and 4 delve into the literature on PR for WECs and OWTs, respectively.
- Section 5 distills key findings from related fields to enhance the understanding of PR in MRE.
- Section 6 provides a synthesis and discussion of the insights gained in the previous Sections.
- Section 7 is the conclusion.

2. Parametric resonance

PR is fundamentally different from the more common structural resonance, as depicted in Fig. 1. The first reports of PR date back to the work of Faraday [1] and Melde [2] in the 19th century. In 1868 Mathieu [3] provided the first mathematical description of PR. PR is now well detailed in classical books [4,5], as well as in modern books [6–8].

In this section, the mathematical foundation for understanding PR is outlined, as follows:

- Section 2.1 presents the canonical Mathieu equation and its extended form, the Hill equation.
- Section 2.2 discusses PR's manifestation in floating structures.
- Section 2.3 details the equations of motion for WECs and OWTs, highlighting where the sources of the time-varying parameters originate.
- Section 2.4 illustrates the concepts discussed, showcasing the occurrence of parametric pitch and roll motions in a spar-buoy oscillating water column (OWC).

2.1. The Hill and Mathieu equations

A general class of second-order homogeneous differential equations with real periodic coefficients for studying PR can be typified by the Hill equation defined as

$$\frac{\mathrm{d}^2u}{\mathrm{d}t^2} + \mu\frac{\mathrm{d}u}{\mathrm{d}t} + a(t)\,u = 0, \tag{1}$$

where u is the dependent variable, μ is the damping coefficient and $a(t)$ is a single-valued periodic function with a fundamental frequency

Nomenclature

Romans

A	Cosine Fourier coefficient
$\mathbf{A}$	Added mass and inertia matrix [kg, kg m/rad], [kg m, kg m^2/rad]
a	Arbitrary periodic function
B	Sine Fourier coefficient
$\mathbf{f}$	Force [N, N m]
g	Gravitational acceleration [m/s^2]
$\mathbf{J}$	Moment of inertia [kg m^2]
m	Mass [kg]
$\mathbf{n}$	Normal to a surface panel
p	Hydrostatic pressure [Pa]
$\mathbf{R}$	Rotation matrix
$\boldsymbol{r}$	Position vector [m]
$\tilde{\boldsymbol{r}}$	Position vector in moving frame [m]
S	Surface [m^2]
t	Time [s]
$\mathbf{T}$	Deviatoric stress tensor [N/m^2]
T	Period [s]
u	Dependent variable in Hill's and Mathieu's equations
$\boldsymbol{v}$	Linear velocity [m/s]
$\mathbf{x}$	Earth-fixed reference frame
$\tilde{\mathbf{x}}$	Moving reference frame
$\mathbf{x}'$	Body-fixed reference frame

Greek symbols

μ	Damping coefficient
ρ	Mass density [kg/m^3]
τ	Dimensionless time
$\boldsymbol{\tau}$	Torque [N m]
$\boldsymbol{\Omega}$	Angular velocity [rad/s]
ω	Frequency [rad/s]

Subscripts

a	Total surface area of the body
B	Center of buoyancy
b	Wetted surface area of the body
exc	Wave excitation
g	Center of gravity
h	Hydrostatic
hs	Hydrostatic restoring
moor	Mooring
p	Pressure
ps	Pressure and shear stresses
PTO	Power Take-OFf
r	Relative to atmosphere
rad	Wave radiation
w	Water
ω	Frequency
∞	Limiting value when $\omega \to \infty$

Acronyms

CFD	Computational Fluid Dynamics
CPU	Central Processing Unit
DoF	Degree of Freedom
FOWT	Floating Offshore Wind Turbine
HPA	Heaving Point Absorber
MRE	Marine Renewable Energy devices
NLFK	Nonlinear Froude–Krylov
OSWC	Oscillating Surge Wave Converter
OWC	Oscillating Water Column
OWT	Offshore Wind Turbine nm
PR	Parametric Resonance
PTO	Power Take-Off
TLP	Tension Leg Platform
TRL	Technology Readiness Level
VIV	Vortex Induced Vibrations
WEC	Wave Energy Converter

of $\omega = 2\pi/T$, see [9]. Under these conditions, $a(t)$ may be written as a Fourier series in the form

$$a(t) = A_0 + \sum_{i=1}^{\infty} A_i \cos(i\omega t) + \sum_{i=1}^{\infty} B_i \sin(i\omega t). \tag{2}$$

The Mathieu equation with damping is a special case where the Fourier series simplifies to

$$a(t) = A_0 + A_1 \cos(\omega t), \tag{3}$$

serving as the foundational example of PR [3]. The Mathieu equation can be rewritten as

$$\frac{\mathrm{d}^2 u}{\mathrm{d}\tau^2} + \frac{\mu}{\omega}\frac{\mathrm{d}u}{\mathrm{d}\tau} + \left(\frac{\omega_\mathrm{n}^2}{\omega^2} + \frac{A_1}{\omega^2}\cos(\tau)\right) u = 0. \tag{4}$$

Here $\tau = \omega t$ is a dimensionless time and $\omega_\mathrm{n}^2 = A_0$, where ω_n is the (undamped) natural resonance condition when $A_1 = 0$. The instability regions of Eq. (4) are depicted in Fig. 2 for different values of μ/ω. This figure shows that there are two regions of instability in the examined frequency range. The first region is around $\omega_\mathrm{n}^2/\omega^2 \approx 1$ for which $\omega \approx \omega_\mathrm{n}$. The second region is centered around $\omega_\mathrm{n}^2/\omega^2 \approx 1/4$, which corresponds to $\omega_\mathrm{n} \approx \frac{1}{2}\omega$. For small values of the parameter A_1, Eq. (4) exhibits PR when the frequency ω is close to the natural frequency of the system or half of it. Fig. 2 also shows that as the damping μ/ω increases, the system is stable for larger disturbance values of A_1/ω^2.

2.2. Parametric resonance in floating bodies

The study of PR floating bodies dates back to Froude [10,11], who describes large roll motions when a ship's roll natural period is twice the heave/pitch natural period. PR in floating bodies typically involves:

- **Wave-induced parameter variation**: Waves act as an external periodic force on floating bodies, causing variation in system parameters such as: buoyancy, stiffness, and mass distribution.
- **Resonance condition**: PR occurs when the wave frequency aligns with a critical frequency and the system starts to 'resonate' with the periodic changes induced by the waves, leading to larger amplitude oscillations.
- **Shift to half frequency**: Upon the onset of PR, the oscillatory motion shifts to a frequency that is half that of the wave frequency. This shift to half frequency is a key indicator of PR.

2.3. Generic equations of motion for WECs and OWTs

The motion of a floating body can be described using the reference frames depicted in Fig. 3. We consider an inertial, earth-fixed reference $\boldsymbol{x} = (x, y, z)$ and a $\tilde{\boldsymbol{x}} = (\tilde{x}, \tilde{y}, \tilde{z})$ reference frame attached to the floating

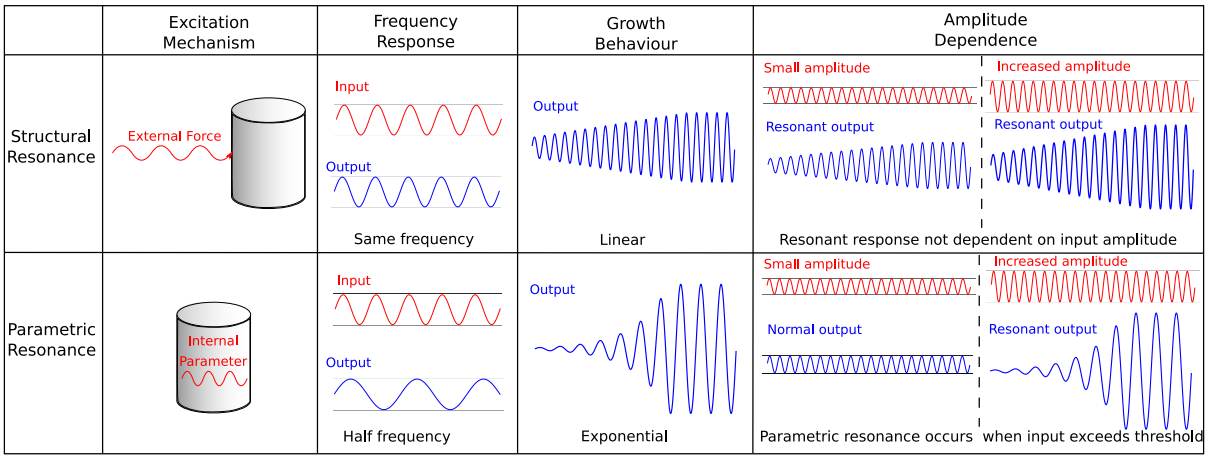

Fig. 1. Comparison of PR with the more commonly known structural resonance. While normal resonance is caused by an external force oscillating at the natural frequency of the structure, leading to a linear increase in structural vibration (until damping limits further growth), PR is caused by an internal oscillation of system parameters, at twice the natural frequency of the structure and with sufficient amplitude, leading to an exponential increase in structural vibration.

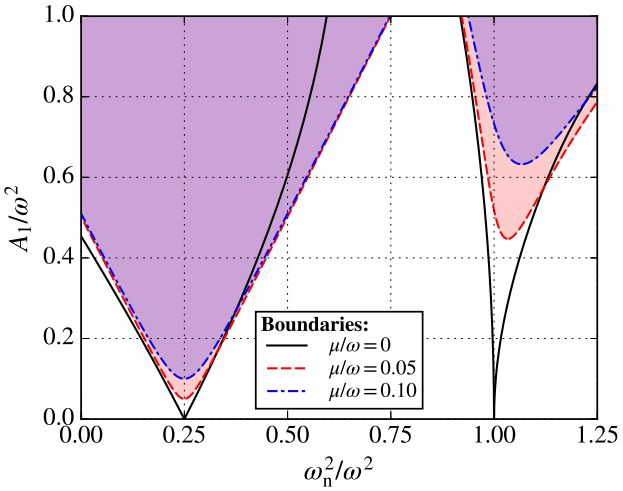

Fig. 2. The region of instability of the damped Mathieu equation for different values of μ/ω.

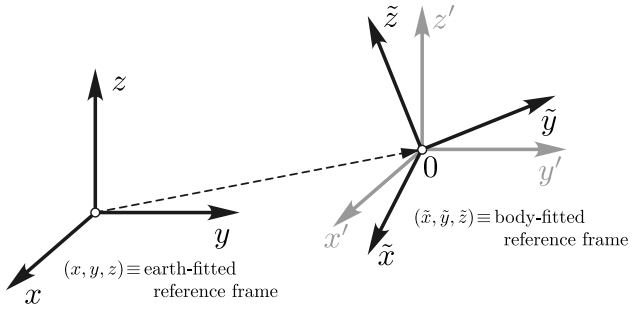

Fig. 3. The $\boldsymbol{x}$ inertial earth-fixed reference frame, the $\boldsymbol{x}'$ body-fixed reference frame, and the $\tilde{\boldsymbol{x}}$ reference frame aligned with the $\boldsymbol{x}$ reference frame and fixed to the body point '0'.

body – the so-called body fixed reference frame – whose motion is defined relatively to the inertial reference frame. We also consider a $\boldsymbol{x}' = (x', y', z')$ reference frame, with axes parallel to the earth-fixed reference frames, whose origin is fixed with respect to the $\tilde{\boldsymbol{x}}$ reference frame. The position and orientation of the body are described relative to the inertial reference frame. The linear and angular velocities of the floating body are described in the body-fixed reference frame.

The position vectors in the $\boldsymbol{x}'$ and $\tilde{\boldsymbol{x}}$ reference frames are related via

$$\boldsymbol{r}' = \mathbf{R}\tilde{\boldsymbol{r}}, \tag{5}$$

where $\mathbf{R}$ is the rotation matrix; see [12]. It can be demonstrated that $\mathbf{R}^{-1} = \mathbf{R}^{\mathsf{T}}$, implying that

$$\tilde{\boldsymbol{r}} = \mathbf{R}^{\mathsf{T}}\boldsymbol{r}'. \tag{6}$$

For simplicity and without loss of generality, we consider the reference point to be the center of gravity of the body $\mathbf{r}_{\mathrm{g}}$, since

$$\int_{S_{\mathrm{a}}} \mathbf{r}_{\mathrm{g}} \times \rho \mathbf{g}\, \mathrm{d}S = 0, \tag{7}$$

where S_{a} is the surface (wetted and non wetted) of the floating body, ρ is the density of the body and $\mathbf{g}$ is the gravitational acceleration.

The coordinates of a point $\boldsymbol{r}'$ in the inertial reference frame are

$$\boldsymbol{r} = \boldsymbol{r}_{\mathrm{g}} + \boldsymbol{r}'. \tag{8}$$

Let $\boldsymbol{v}$ and $\boldsymbol{\Omega}$ be the linear and angular velocities defined in the $\boldsymbol{x}$ reference frame and expressed in the $\tilde{\boldsymbol{r}}$ reference frame as $\tilde{\boldsymbol{v}} = \mathbf{R}^{\mathsf{T}}\boldsymbol{v}$ and $\tilde{\boldsymbol{\Omega}} = \mathbf{R}^{\mathsf{T}}\boldsymbol{\Omega}$. The balance of momentum and angular momentum written in the $\tilde{\boldsymbol{r}}$ reference frame reads

$$\begin{aligned} m\dot{\tilde{\boldsymbol{v}}}_{\mathrm{g}} + \boldsymbol{\Omega} \times \tilde{\boldsymbol{v}}_{\mathrm{g}} &= \mathbf{R}^{\mathsf{T}}\left(m\boldsymbol{g} + \boldsymbol{f}_{\mathrm{ps}}(t) + \boldsymbol{f}_{\mathrm{PTO}}(t) + \boldsymbol{f}_{\mathrm{moor}}(t)\right), \\ \tilde{\mathbf{J}}(t)\,\dot{\tilde{\boldsymbol{\Omega}}} + \boldsymbol{\Omega} \times \left(\tilde{\mathbf{J}}(t)\,\tilde{\boldsymbol{\Omega}}\right) &= \mathbf{R}^{\mathsf{T}}\left(\boldsymbol{\tau}_{\mathrm{ps}}(t) + \boldsymbol{\tau}_{\mathrm{PTO}}(t) + \boldsymbol{\tau}_{\mathrm{moor}}(t)\right), \end{aligned} \tag{9}$$

Here m is the mass and $\tilde{\mathbf{J}}$ is the moment of inertia of the body in the $\tilde{\boldsymbol{x}}$ reference frame, $\boldsymbol{f}_{\mathrm{PTO}}$ and $\boldsymbol{\tau}_{\mathrm{PTO}}$ are the force and torque exerted on the body by the PTO, $\boldsymbol{f}_{\mathrm{moor}}$ and $\boldsymbol{\tau}_{\mathrm{moor}}$ are the force and torque exerted on the fairlead by the mooring lines.

If the moment of inertia is time dependent, it can be decomposed as

$$\tilde{\mathbf{J}}(t) = \tilde{\mathbf{J}}_0 + \Delta\tilde{\mathbf{J}}(t), \tag{10}$$

a time-constant term $\tilde{\mathbf{J}}_0$ plus a time-variation function of $\Delta\tilde{\mathbf{J}}(t)$.

The force $\boldsymbol{f}_{\mathrm{ps}}(t)$ is the resultant of the pressure and shear stresses

$$\boldsymbol{f}_{\mathrm{ps}}(t) = -\oint_{S_{\mathrm{b}}(t)} p_{\mathrm{r}}(\boldsymbol{r}', t)\boldsymbol{n}\, \mathrm{d}S, + \oint_{S_{\mathrm{b}}(t)} \mathbf{T}(\boldsymbol{r}', t)\boldsymbol{n}\, \mathrm{d}S, \tag{11}$$

where p_{r} is the static pressure relative to the atmosphere, $\mathbf{T}$ is the deviatoric stress tensor, $\boldsymbol{n}$ is the body's surface normal, and S_{b} the wetted surface of the body. Hereinafter, it is assumed that the pressure and shear stresses in the air are negligible compared to the wetted boundary. The torque vector $\boldsymbol{\tau}_{\mathrm{ps}}(t)$ resulting from the pressure and

shear stresses is

$$\boldsymbol{\tau}_{\mathrm{ps}}(t) = -\oint_{S_{\mathrm{b}}(t)} \boldsymbol{r}' \times p_{\mathrm{r}}(\boldsymbol{r}', t)\, \boldsymbol{n}\, \mathrm{d}S + \oint_{S_{\mathrm{b}}(t)} \boldsymbol{r}' \times \left(\mathbf{T}(\boldsymbol{r}', t)\, \boldsymbol{n}\right) \mathrm{d}S. \tag{12}$$

It should be noted that $p_{\mathrm{r}}(\boldsymbol{r}', t)$ is the pressure field that results from the fluid–structure interaction with the floating body and not simply the pressure field from the waves in the absence of the floating body. The pressure and shear stress fields can be computed using numerical wave tanks based on computational fluid dynamics (CFD) solvers [13].

2.3.1. Equations of motion under the linear wave theory

The equations of motions under the linear wave theory are the most common model used to study PR due to its simplicity and reasonable agreement with experimental data. The balance of momentum and angular momentum written in the $\tilde{\boldsymbol{r}}$ reference frame reads

$$\begin{aligned} \left(m\mathbf{I} + \mathbf{A}_{\infty}\right) \dot{\tilde{\boldsymbol{v}}}_{\mathrm{g}} + \boldsymbol{\Omega} \times \tilde{\boldsymbol{v}}_{\mathrm{g}} &= \mathbf{R}^{\top}\left(\boldsymbol{f}_{\mathrm{exc}}(t) + \boldsymbol{f}_{\mathrm{rad}}(t) + \boldsymbol{f}_{\mathrm{hs}}(t) + \boldsymbol{f}_{\mathrm{PTO}} + \boldsymbol{f}_{\mathrm{moor}}\right), \\ \left(\tilde{\mathbf{J}}(t) + \mathbf{A}_{\infty}\right) \dot{\tilde{\boldsymbol{\Omega}}} + \boldsymbol{\Omega} \times \left(\tilde{\mathbf{J}}(t)\, \tilde{\boldsymbol{\Omega}}\right) &= \mathbf{R}^{\top}\left(\boldsymbol{\tau}_{\mathrm{exc}}(t) + \boldsymbol{\tau}_{\mathrm{rad}}(t) + \boldsymbol{\tau}_{\mathrm{hs}}(t) + \boldsymbol{\tau}_{\mathrm{PTO}} + \boldsymbol{\tau}_{\mathrm{moor}}\right). \end{aligned} \tag{13}$$

Here $\mathbf{I}$ is the 3×3 identity matrix, $\mathbf{A}_{\infty}$ is the added mass and inertia matrix in the limit as the frequency goes to infinity, $\boldsymbol{f}_{\mathrm{exc}}(t)$ and $\boldsymbol{\tau}_{\mathrm{exc}}(t)$ are the excitation force and torque vectors, $\boldsymbol{f}_{\mathrm{hs}}(t)$ and $\boldsymbol{\tau}_{\mathrm{hs}}(t)$ are the hydrostatic restoring force and torque vectors, $\boldsymbol{f}_{\mathrm{rad}}(t)$ and $\boldsymbol{\tau}_{\mathrm{rad}}(t)$ are the radiation force and torque vectors. These matrices and vectors are usually computed based on hydrodynamic coefficients computed using boundary element method codes [14–18]. Some of these codes required a translation of the hydrodynamic coefficients to the center of mass, see [19] for further details.

Linear wave theory assumes irrotational flow and, as such, the shear stresses are zero. Under a hydrostatic pressure field p_{h} (still water conditions), the resultant of the pressure force, $\boldsymbol{f}_p$, is equal to minus the weight of the displaced water volume $\forall$, thus giving

$$\boldsymbol{f}_p(t) = -\oint_{S_{\mathrm{b}}(t)} p_{\mathrm{h}}(\boldsymbol{r}', t)\, \boldsymbol{n}\, \mathrm{d}S = \rho g \forall(t)\, \boldsymbol{e}_z, \tag{14}$$

For the current purpose of studying PR, the displaced volume can be decomposed as

$$\forall(t) = \forall_0 + \Delta\forall(t), \tag{15}$$

where $\forall_0$ is the displaced volume in still water conditions and $\Delta\forall(t)$ is a smaller time variation term. The resultant momentum is

$$\boldsymbol{\tau}_p(t) = -\oint_{S_{\mathrm{b}}(t)} \boldsymbol{r}' \times p_{\mathrm{h}}(\boldsymbol{r}', t)\, \boldsymbol{n}\, \mathrm{d}S = \boldsymbol{r}'_{\mathrm{B}}(t) \times \left(\rho_{\mathrm{w}} g \forall(t)\, \boldsymbol{e}_z\right), \tag{16}$$

where $\boldsymbol{r}'_{\mathrm{B}}$ is the center of buoyancy defined as the center of mass of the displaced water volume $\forall$, which is time varying. The hydrostatic restoring force and moment are therefore

$$\boldsymbol{f}_{\mathrm{hs}}(t) = \left(-m + \rho_{\mathrm{w}} \forall(t)\right) g\, \boldsymbol{e}_z, \tag{17}$$

and

$$\boldsymbol{\tau}_{\mathrm{hs}}(t) = \boldsymbol{r}'_{\mathrm{b}}(t) \times \left(\rho_{\mathrm{w}} g \forall(t)\, \boldsymbol{e}_z\right). \tag{18}$$

2.4. Example

In Eqs. (9) and (13), PR may arise from the time variation of the inertia matrix $\tilde{\mathbf{J}}$ and the instantaneous wetted area. Variation of the wetted area is the most common cause of PR for floating bodies, as demonstrated in the following example. For this case, in normal operation, the spar buoy should predominately heave, with a small amount of pitch and very little to no roll due to the axisymmetry. However, the wave-induced heave motion causes the instantaneous wetted area to change as the spar-buoy oscillates into and out of the water, which shifts the center of buoyancy, as depicted in Fig. 4. The shifting center of buoyancy results in a time-variable hydrostatic stiffness for pitch and roll motions, Eq. (18). This time-varying hydrostatic stiffness in Eq. (13) acts similarly to the $a(t)$ term in Eq. (1), potentially triggering PR in pitch and roll when the oscillation amplitudes are sufficiently large and the damping relatively low, as illustrated in Fig. 2.

The behavior of the spar-buoy, as depicted in Figs. 5 and 6 from experiments outlined in [20], illustrates the dynamics under normal conditions and during PR. Normally, pitch oscillations are minor and synchronize with the wave period, accompanied by negligible roll motion. In contrast, PR significantly amplifies pitch oscillations, increasing their amplitude by an order of magnitude with a period twice that of the waves. Similarly, pronounced roll motions emerge, also with a period twice that of the waves. This demonstrates PR's effect in generating large-amplitude oscillations at half the wave frequency.

3. Parametric resonance in WECs

The literature pertaining to PR in WECs can be grouped into four main categories:

- Section 3.1 Observation - Publications noting the existence of PR when it was not intended.
- Section 3.2 Suppression - Publications aiming mitigate the existence of PR.
- Section 3.3 Exploitation - Publications aiming to utilize the existence of PR to increase the energy capture of a WEC.
- Section 3.4 Modeling - Publications aiming to investigate PR through modeling.

3.1. Observation

Many studies unintentionally encountered PR, either in physical testing or simulations, as detailed in Table 1. The first recorded instance of PR in WECs was during late-1980s wave tank experiments on the Frog [22], a point absorber designed for heave, where intense pitch oscillations were observed at half the wave frequency.

3.1.1. Wave regularity

PR is most frequently reported under regular waves, where periodic excitation aligns with system natural frequencies. Giassi et al. [41–43] perform the same tests in regular and irregular waves and note that the dynamic instability mostly occurred for regular waves. While the impact of irregular waves on the occurrence of PR is discussed more in Section 3.3.7, in general the study of PR in irregular waves is a knowledge gap requiring more attention, as discussed in Sections 6.1 and 6.2.

3.1.2. WEC types

The observation of PR spans multiple WEC designs:

Oscillating Water Columns: For fixed, shoreline-based systems, PR is observed in the sloshing mode of the water column [23]. For heaving spar-type designs [29–34], parametric pitch/roll is observed (as in Section 2.4). The occurrence of PR in OWCs leads to unexpected oscillations that reduce energy capture and challenge linear hydrodynamic models.

Two-body Heaving Point Absorbers: The floating OWCs [29–34] are an example of a two-body HPA, comprising the outer spar-buoy and the inner water column. Other two-body HPAs [22,35,39] also experienced similar parametric pitch/roll resonance. The coupled dynamics of the two-bodies may be a trigger for PR, thus the decoupling of the two bodies is explored as a suppression strategy in Section 3.2.

Mooring Influences: WECs whose PTOs act through the moorings exhibited PR in lateral DoFs [26–28,36,41–43]. For some of these [26,27] the occurrence of PR is noted as being dependent on the PTO settings such as damping or hydraulic pressure. For some point absorbers with tri-point moorings [24,40], parametric yaw motion was triggered when parametric roll occurred.

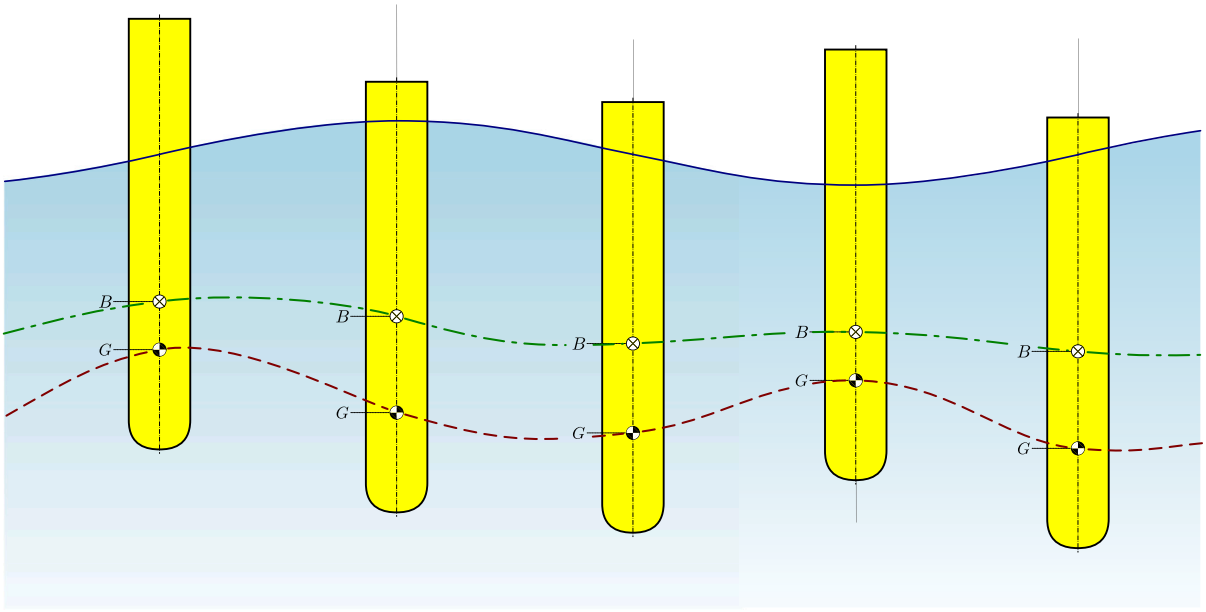

Fig. 4. The center of buoyancy, B, and the center of gravity G shift due to heave motion The two points do not follow the same path.

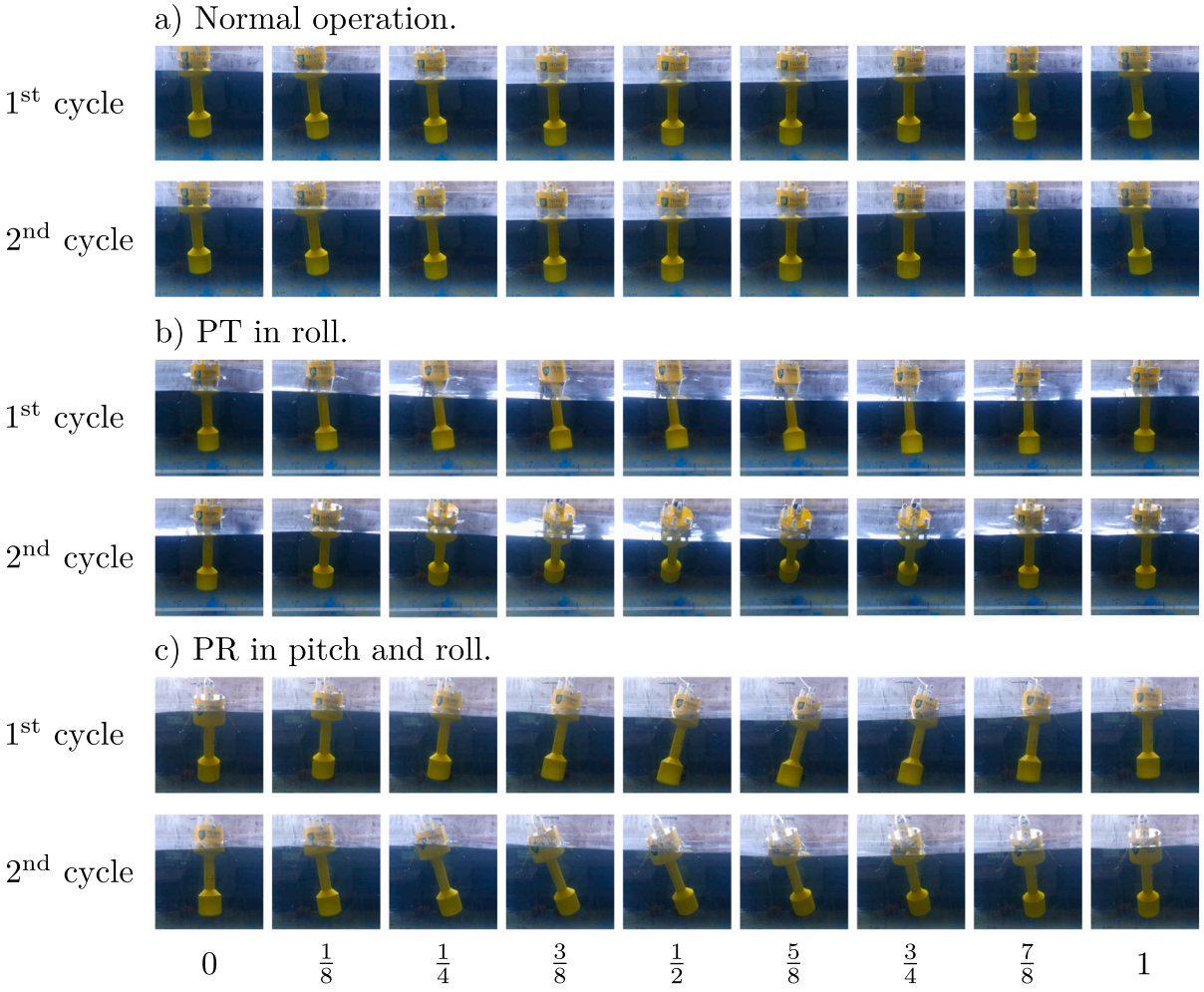

Fig. 5. The motion of an OWC Spar buoy over one wave period, for two consecutive cycles, for the case of (a) normal operation, (b) PR in Roll and (c) PR in Pitch and Roll. See videos at [21].

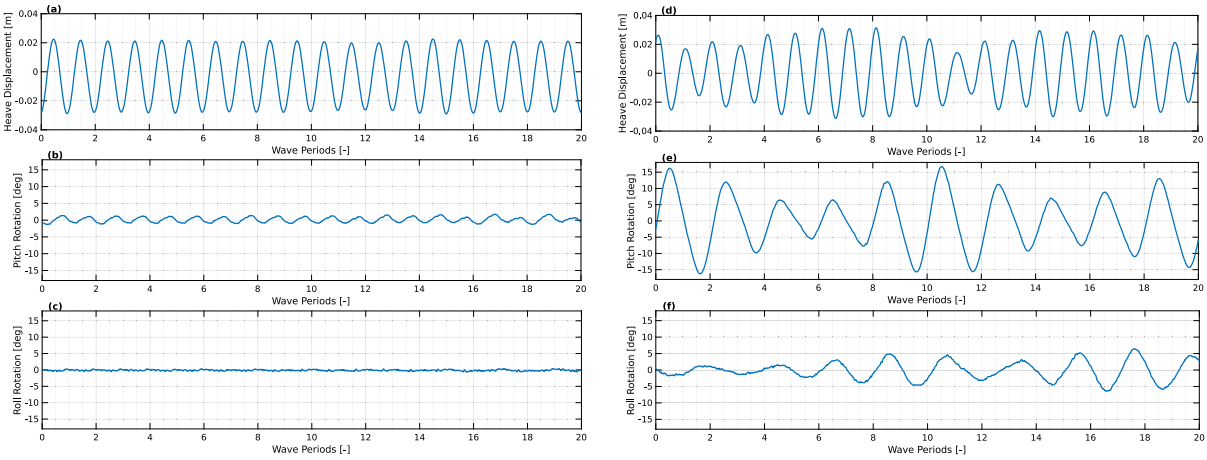

Fig. 6. Time series for a normal operation case: (a) Heave, (b) Pitch and (c) Roll, and for a PR case: (d) Heave, (e) Pitch and (f) Roll.

Table 1
Publications not explicitly studying PR, but observe its occurrence in WECs.

Ref.	WEC	Waves	Instability	Experiment
[22]	*The FROG*	Regular	Pitch	Wave tank
[23]	LIMPET OWC	Regular	Slosh	Wave tank
[24]	*SEAREV*	Regular + Spectrum	Roll + Yaw	Wave tank
[25]	Sloped WEC	Regular	Roll	Wave tank
[26]	Spring Reel Tethered Buoy	Regular	Sway	Wave tank
[27]	*SurfPower*	Regular	Sway	Simulation
[28]	*Manchester Bobber*	Regular	Surge	Wave flume
[29]	Floating cylindrical OWC	Regular	Roll	Wave tank
[30–34]	*OWC Spar Buoy*	Regular	Pitch + Roll	Wave flume
[35]	Two-body HPA	Regular	Pitch + Roll	Wave tank
[36]	*CETO 6*	Regular	Sway and roll	Wave tank
[37]	*Three tether WEC*	Spectrum	Pitch	Simulation
[38]	HPA	Regular	Pitch	Simulation
[39]	Two-body HPA	Regular + Spectrum	Pitch	Wave tank
[40]	*Floating Power System*	Spectrum	Roll + Yaw	Wave tank
[41–43]	Taut-moored point absorber	Regular + Spectrum	Sway	Wave tank

Table 2
Review of publications investigating control methods to suppress PR in WECs.

Ref.	WEC	Waves	Instability	Control
[27]	*SurfPower*	Regular + Spectrum	Sway	Hydraulic pressure in PTO to adjust the mooring stiffness
[44]	*WaveBob*	Regular	Roll	Notch filter in PTO coupling between the two bodies
[35]	2-body HPA	Regular	Pitch + Roll	Fins
[45]	*SEAREV*	Regular + Spectrum	Roll	Geometric optimization
[46]	2-body HPA	Regular	Pitch + Roll	Mooring system
[47]	OWC Spar Buoy	Regular	Pitch + Roll	Fins
[48]	OWC Spar Buoy	Regular	Pitch + Roll	Geometric optimization
[49]	*Variable Inertia System WEC*	Regular	Roll	Changing the moment of inertia to shift the resonance frequency
[20]	OWC Spar Buoy	Regular	Pitch + Roll	Relief valve to decouple the buoy and water column

3.1.3. Implications for energy capture and modeling

Two main challenges are seen to arise for WECs due to PR:
Reduced Power Output: PR diverts energy from the primary power-generating DoF to secondary modes, reducing the overall efficiency.
Modeling Discrepancies: Many studies noted mismatches between numerical models and experimental results when PR occurred, emphasizing the need for higher-fidelity modeling. Notably, 13 of the 16 cases in Table 1 stem from physical experiments, suggesting that many WEC models may inadequately capture PR and are unable to predict its occurrence.

3.2. Suppressing parametric resonance

Table 2 compiles publications on PR suppression. The control methods can be divided into two categories: passive and active.

3.2.1. Passive mechanisms

Passive controls like fins or strakes enhance hydrodynamic damping in pitch/roll, effectively reducing PR in spar platforms [50]. Beatty et al. [35] demonstrate that strakes could mitigate pitch and roll and improve power output at PR frequencies. Ortiz [46] explored mooring dynamics as an additional form of passive control. Gomes et al. [47] applied large fins to the OWC Spar Buoy, depicted in Fig. 7(a), decreasing but not fully eliminating PR-triggered pitch and roll oscillations. Cordonnier et al. [45] and Gomes et al. [48] took a different route by optimizing WEC design from the outset to avoid PR, concluding that optimal designs accounting for PR tend to be wider.

3.2.2. Active control

Active control strategies directly alter WEC dynamics to counteract PR. Nicoll and Wood [27] modify mooring line tension through hydraulic PTO pressure to offset PR in the SurfPower WEC, Fig. 7(b). Villegas and van der Schaaf [44] combat PR in the WaveBob utilizing

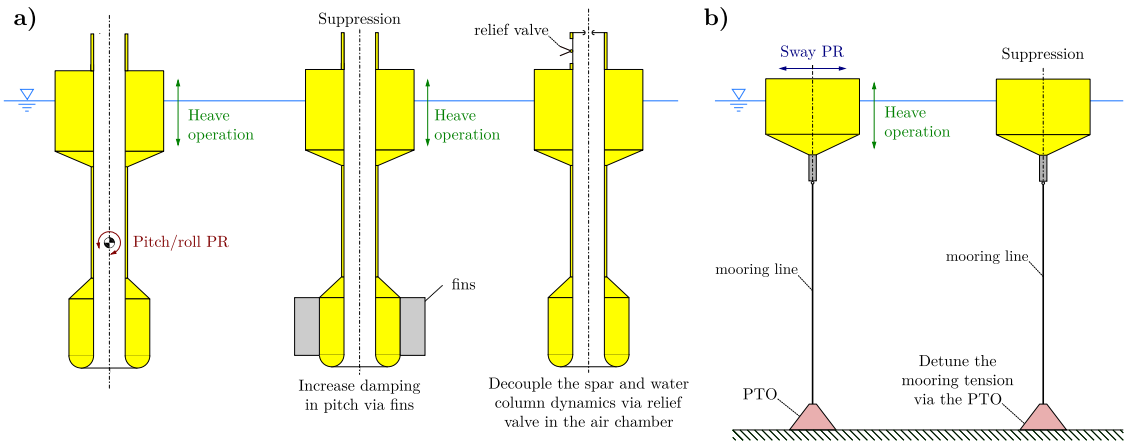

Fig. 7. Mitigation of PR by: (a) adding fins to increase damping or using a relief valve to alter the roll and pitch natural frequencies, (b) adjusting the mooring line tension via the hydraulic pressure in the PTO.

Table 3
Comparative analysis of PR suppression strategies in WECs.

Strategy	Implementation cost	Maintenance requirements	Effectiveness	Impact on primary power capture
Fins/strakes [35,47]	Low	Low	Low	Minor negative
Geometric optimization [45,48]	None	None	High	Minor negative
Mooring (Passive) [46]	Medium	Medium	Medium	Minor negative
Mooring (Active) [27]	Low	Low	High	Negligible
Decoupling bodies [20,44]	Medium	Medium	High	Minor negative
Variable inertia [49]	High	High	Mixed	Potentially positive

a notch filter to negate PTO forces at PR frequencies. Maloney [49] employ an internal, elastically supported mass within a WaveBob-like HPA, to adjust the spar's natural frequency. Davidson et al. [20] use a relief valve in the OWC Spar Buoy's air chamber to change its dynamics, depicted in Fig. 7(a). Since active controllers switch on when required and remain inactive during normal operation, they require real-time monitoring and early warning systems for the onset of PR, as shown in [51].

3.2.3. Comparative analysis of suppression strategies

Except for one study [27], the suppression of PR focused on pitch/roll motions in spar-type WECs. A comparison of PR suppression strategies is presented in Table 3.

Passive approaches offer advantages in terms of reliability and maintenance. Geometric optimization stands out as the most cost-effective solution, requiring no additional components, however may result in a geometric design which is suboptimal in terms of power production. Fins and strakes offer moderate effectiveness with minimal maintenance, though may introduce additional drag to the primary DoF that slightly reduces power capture. It is also worth mentioning that laboratory scale results may overestimate the effect of fins due to the small Reynolds number. Active control strategies demonstrate promising PR suppression capabilities but at the cost of increased complexity and the risk of controller malfunction.

3.3. Exploiting parametric resonance

The earliest study to exploit PR for wave energy conversion is from 1995 [52], considering a parallel plate capacitor, immersed in water, combined with an oscillating electromagnetic circuit. Waves passing through the plates vary the capacitance, and parametrically excite oscillations in the circuit. Several other strategies to exploit PR have been investigated in the past two decades and are collated in Table 4. While many of these strategies leverage the hydrodynamic PR phenomena in DoFs such as heave, pitch, roll and OWC motion (denoted in the *Instability* column in Table 4), others aim to exploit mechanical PR via the rotation of a pendulum.

3.3.1. OWC volume

Olvera et al. [53] exploit PR in an OWC by varying the OWC chamber volume. A controllable valve is connected to an auxiliary chamber, which increases the volume and reduces the air spring's restoring force. Simulations demonstrate that PR yields maximal system response, maintaining large oscillations even if the input frequency shifts, diverging from typical resonance behavior.

3.3.2. Mass-modulation

Mass-modulation in a two-body HPA is proposed in [73–78] by varying one body's inertia with each wave cycle, leveraging hydrodynamic added mass and control valves. Initial simulations by Orazov et al. [73,75] demonstrated a 25%–65% increase in energy output and reduced damping sensitivity with mass-modulation. Further analysis explored stability and energy potential, with Rougirel [76] validating the scheme's efficiency over traditional oscillators. Orazov's thesis [74] and subsequent improvements by Diamond et al. [77,78] addressed momentum loss and refined the model, respectively, showing up to a 200% boost in energy output and enabling passive flap operations through a refined mass-modulation strategy.

3.3.3. Parametrically excited pendula

Dotti et al. [89] delved into the nonlinear dynamics of WEC pendulum systems, emphasizing the potential of the rotational motion of the vertical parametric pendulum for energy harvesting, depicted in Fig. 8(a). Research at the University of Aberdeen [54–58,63] and furthered by Heriot-Watt University [61,62,64–68,70] has delved into harmonic excitation, non-sinusoidal wave profiles, and stochastic forcing to understand and enhance pendulum energy capture under various conditions.

Addressing oceanic low-frequency waves necessitating long pendulums (Fig. 8(b)), [62,63] propose and experimentally validates an innovative N-pendulum system, boasting a length-independent and tunable

Table 4
Review of publications exploiting PR in WECs.

Ref.	WEC	Waves	Instability	Control
[52]	Immersed capacitor	Regular	AC circuit	Time varying capacitance
[53]	Shore based OWC	Regular	OWC	Time varying air chamber volume
[54–72]	Pendulum on HPA	Reg. + Spectrum	Pendulum rotation	Parametric excitation of the pendulum
[73–78]	Two-body HPA	Regular	Heave	Time varying inertia
[79]	Vessel with horizontal pendulum	Regular	Roll	Pitch-roll coupling of hull to induce large rotation of internal pendulum
[80–82]	3 DoF Cylinder	Reg. + Spectrum	Pitch	Energy maximizing model predictive control
[83]	HPA	Regular	Heave	Leveraging heave-to-heave PR
[84]	UGEN	Reg. + Spectrum	Roll	Leveraging parametric roll
[85]	HPA	Regular	Heave	Time-varying PTO damping
[86]	Vertical Axis Parametric Pendulum	Reg. + Spectrum	Pendulum rotation	Parametric excitation of the pendulum
[87,88]	The PeWEC	Regular	Pitch	Leveraging parametric roll

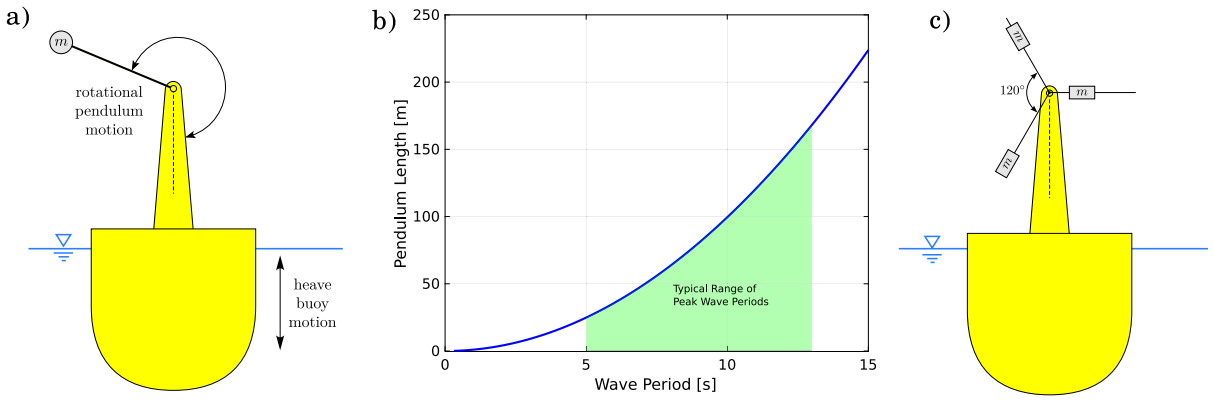

Fig. 8. (a) The vertical parametric pendulum type WEC. (b) The required pendulum length to align the natural period at twice a typical wave period [90]. (c) The tri-pendulum concept whose natural period can be tuned by adjusting the position of the masses, eliminating the requirement of excessively long pendula.

natural frequency, depicted in Fig. 8(c). [70] also developed a method to adjust natural frequencies to changing wave conditions by altering the pendulum's inclination angle. Subsequent studies integrated WEC hydrodynamics with pendulum dynamics, observing that WEC dynamics filtered the 'noise' in stochastic wave inputs, enhancing pendulum rotation [64] and identifying vast regions in the wave frequency/amplitude space with a high likelihood of inducing rotation [71,72]. The potential benefits of multiple counter-rotating pendulums are highlighted in [57]. Experimental validations in [59,60] note discrepancies between experimental and theoretical rotation ranges.

Recently, Jiang et al. [86] consider a Vertical Axis Parametric Pendulum WEC, showing a jump in the output power by an order of magnitude when the pendulum enters the PR region.

3.3.4. Parametric pitch/roll motion

While Section 3.2 focuses on reducing pitch/roll motions, some studies aim to leverage these instabilities for greater power capture. Yerrapragada et al. [79] design a floating vessel with an internal pendulum that exploits parametric roll for increased energy yield. The work in [80–82] considers a point absorber, equipped with a theoretical PTO able to apply forces in heave, surge and pitch. Under this assumption, the parametric coupling between DoFs is leveraged to maximize the power output using time-varying linear quadratic Gaussian control [82], model predictive control [81] and pseudo-spectral control [80]. Silva et al. [84] report on the UGEN, which is inspired by the U-shaped tanks for ship roll stabilization, drawing on their experience with parametric roll in shipping [91–93]. Similarly, Giorgi [87,88] designs a pitching WEC with a 2:1 ratio between heave and pitch natural frequencies in order to leverage PR to increase the WECś bandwidth.

3.3.5. Parametric heave motion

Lelkes et al. [83] suggest leveraging heave-to-heave PR to improve energy capture in a HPA. Spars with sloped hull surfaces near the waterline can exhibit this PR due to the variation in waterplane area during heave oscillations. Haslum et al. [94] noted in 1999 that the heave response was 20 times larger than frequency domain model predictions at PR frequencies, with a detailed study in Haslum's PhD thesis [95]. Jiang et al. [96,97] analyze Arctic spars with sloped hulls designed for ice-breaking, examining both heave–heave and heave–pitch PR.

3.3.6. Time-varying damping

Giorgi et al. [85] show that oscillating the PTO's damping coefficient at double the frequency of the sinusoidal excitation force induces PR, greatly widening the response bandwidth. Of interest, Billah [98] argues that "...parametric excitation is only possible when an energy-storing parameter like inertia and/or stiffness (and not damping) changes periodically". However, the application of time-varying damping at twice the excitation frequency has also been applied to vibration energy harvesting, where it is also referred to as exploiting PR [99,100].

3.3.7. Comparative analysis of PR exploitation strategies

A comparative analysis of approaches to exploit PR in WECs is synthesized in Table 5.

Passive vs. Active: Alhough systems that leverage parametric pitch/roll motion are generally passive, active control forces from the PTO can also be employed to drive the system along desired trajectories [80–82]. However, active PTO controls such as this, as well as time-varying damping [85], rely on accurate knowledge of wave excitation forces, posing additional practical challenges. Similarly, although

Table 5
Comparative analysis of PR exploitation strategies in WECs.

Strategy	Implementation complexity	Maintenance requirements	Technology readiness	Control
Mass modulation	High	High	Low	Active
OWC volume	High	Medium	High	Active
Pendulum systems	Medium	Medium	Medium	Passive[a]
Parametric pitch/Roll	Low	Medium	High	Passive[a]
Parametric heave	Low	Low	High	Passive
Time varying damping	Medium	Low	High	Active

[a] Denotes potential for active control.

pendulum systems passively leverage parametric excitation, active control methods have also been proposed, such as providing additional electromechanical vertical oscillations [61] or using a telescopic mechanism to dynamically adjust the pendulum length [69]. On slower timescales, adjusting pendulum lengths to tune their natural frequency to changing sea states is suggested [62].

Technology Readiness and Practical Considerations:

High readiness: Systems exploiting hydrodynamic coupling-induced instabilities in pitch, roll, or heave DoFs require no special technologies beyond existing WEC design methodologies. Time-varying damping and OWC volume variation rely on relatively mature subsystems (e.g., controllable PTOs or air chambers) with straightforward control loops. These approaches can likely be implemented with minimal additional development.

Medium readiness: Pendulum-based systems have been validated in numerous lab-scale mechanical shaker type experiments, but their integration at full scale — especially on a floating body in irregular seas — remains a challenge.

Low readiness: Mass-modulation, while theoretically promising, remains largely confined to small-scale or numerical demonstrations. This approach requires complex fluid-handling systems that may encounter reliability and efficiency challenges in real-sea environments.

Regular vs. Irregular Waves: Most approaches demonstrate strong potential in *regular* wave conditions, where the timing of parametric excitation is easier to maintain. However, extending these strategies to *irregular* or multi-directional wave conditions introduces additional complexities. Active methods benefit from advanced controllers that can adapt in real-time, thus sustaining parametric gains over more complex spectra. Since PR is particularly sensitive to the excitation frequency, Giorgi [88] examines the *instantaneous frequency* of irregular waves and find that PR is dependent on the time-variability of the instantaneous frequency. The onset of PR requires the instantaneous frequency to be a twice the natural frequency of the relevant DoF for a sustained amount of time, and when it deviates from this frequency then the PR response rapidly diminishes.

Reliability: While PR-based strategies amplify oscillations and enhance energy capture, they also raise concerns regarding fatigue, structural loading, and maintenance. Large cyclic stresses on moorings, PTO linkages, or structural components could compromise long-term reliability. Similarly, systems with high mechanical complexity, may introduce additional failure points. Future work should focus on assessing the trade-offs between improved energy capture and increased wear on WEC components.

3.4. Modeling parametric resonance

WEC dynamics can be represented by the 2nd order ODE, Eq. (13). In conventional WEC models [101,102], each term in Eq. (13) is a linear, time-invariant function (allowing frequency domain analysis). This section reviews methods to incorporate time-variation into these terms to model PR for WECs. Modeling the influence of mooring systems on PR is also discussed. Table 6 compile studies that use mathematical models to explore PR.

3.4.1. Time-varying restoring force

Introducing time-variation to the restoring term in Eq. (13), resembles the damped and forced Mathieu equation. [79] employ a model from shipping [117], that captures the pitch/roll coupling through a roll restoring torque term that is dependent on the pitch position. Similarly, [47,48] use a shipping method [118] to formulate a Mathieu equation for predicting PR in the OWC Spar Buoy. Considering a simple cylinder, [80–82] employ geometric analysis to calculate buoyancy and gravity centers from heave and pitch movements, to derive a variable pitch restoring torque term via Taylor expansion. [39,119,120] devise a time domain model with a pitch restoring torque coefficient contingent on the immediate buoyancy center position. [51] employ a model with a time-varying pitch restoring coefficient, tailored for a cylindrical spar buoy [121]. [112] use system identification methods [122] to model the restoring force/torque based on heave and pitch displacement.

3.4.2. Time-varying inertia

[73–78] model the mass modulation scheme in Section 3.3.2 with a piece-wise linear model. [73–76] use a simple 1 DoF mass–spring–damper system and add/subtract a mass each quarter wave cycle. However, [74] highlights deficiencies in this simplistic model. [77] identifies that adding/subtracting mass is equivalent to an impulsive force, resulting in momentum loss; thus, extend the model with an impulse term. [78] further extends to two DoFs and more realistic hydrodynamics.

Displacements measured in the inertial frame, but forces and velocities measured in the body-fixed frame (a time-varying axis), is accounted via a kinematic mapping to the inertia matrix in [123], resulting in Coriolis and centripetal forces. Similarly, [120] model inertia forces up to 2nd-order in the body motions, resulting in centripetal forces and mass matrix elements varying with the body displacement. Of note, both studies observe large yaw instabilities when PR in pitch/roll occurs.

3.4.3. Time-varying excitation force

[114] add parametric excitation into a spectral domain model for an Oscillating Surge Wave Converter (OSWC), building on [124], where the excitation force parameters are modulated by the OSWC's flap angle. [83] pre-calculate excitation force coefficients for various body displacements and use polynomial fits to model the force as a function of displacement. Simulation results for a HPA are shown to align closely with those from a Nonlinear Froude–Krylov (NLFK) force model but are computationally four orders of magnitude faster. This method is extended to 2 DoF in [125].

3.4.4. Nonlinear Froude–Krylov force

The NLFK force is calculated, at each timestep, by integrating the pressure from the undisturbed wave over the instantaneous wetted surface. [103] demonstrate the NLFK model can predict parametric roll and yaw in the SEAREV not captured by linear models, but motions are exaggerated due to no viscosity. [104,105] demonstrate its accuracy in predicting PR onset and oscillation magnitudes for the Wavebob. [35,46,49] also employed the NLFK approach for a Wavebob-like two-body HPA. For axisymmetric WECs, [126] propose an efficient analytical integration method, cutting runtime by nearly fourfold, and

Table 6
Review of publications modeling PR in WECs.

Ref.	WEC	Waves	Model	Instability	Analysis
[103]	*SeaREV*	Regular	NLFK	Roll	Assess models for PR
[27]	*SurfPower*	Regular	Pendulum equation	Sway	Predict PR frequencies
[73–78]	Two-body HPA	Regular	Time-varying inertia	Heave	Assess control method to exploit PR
[79]	Horizontal pendulum in vessel	Regular	Time varying restoring	Roll	Assess control method to exploit PR
[35,49]	2-body HPA	Regular	NLFK	Pitch + Roll	Assess control method to suppress PR
[104]	*WaveBob*	Regular	NLFK	Pitch + Roll	Develop model for PR
[105]	*WaveBob*	Regular	NLFK	Pitch + Roll	Compute limits of stability
[46]	2-body HPA	Regular	NLFK + Lumped mass mooring	Pitch + Roll	Assess control to suppress PR
[47,48]	*OWC Spar Buoy*	Regular	Time varying restoring	Pitch + Roll	Identify regions of instability
[36,106]	*CETO 6*	Regular + Spectrum	2nd Order Taylor Series for mooring	Sway + Roll	Anaylse transverse motion instability
[107]	3 tethered *CETO*	Regular + Spectrum	2nd + 3rd Order Taylor Series for mooring	Yaw	Onset and limiting amplitude of yaw instability
[108]	*CorPower*	Regular	NLFK	Pitch + Roll	Assess efficient PR models
[109]	*WaveBob*	Regular	NLFK	Pitch + Roll	Assess efficient PR models
[109,110]	*OWC Spar buoy*	Regular + Spectrum	NLFK	Pitch + Roll	Assess efficient PR models
[80–82]	3 DoF Cylinder	Regular + Spectrum	Time varying restoring	Pitch	Energy maximizing control algorithms
[39]	2-body HPA	Regular	Time varying restoring	Pitch + Roll	Extend model to capture PR
[111]	HPA Cylinder	Regular	RANS + Euler	Pitch + Roll	Simulating PR with CFD
[112]	HPA Cylinder	Regular	Time varying restoring	Pitch	Using system identification to model PR
[113]	*OWC Spar buoy*	Regular	NLFK + Quasi-static mooring	Pitch + Roll	Effect of mooring parameters on PR
[114]	OSWC flap	Spectrum	Modulated excitation force	Flap rotation	Include PR in spectral domain model
[51]	HPA Cylinder	Regular + Spectrum	Time varying restoring	Pitch	Assess system for the real-time detection of PR
[115,116]	HPA Cylinder	Regular	NLFK	Pitch + Roll	Examine energy transfer during PR
[83]	HPA Cylinder	Regular	Time varying excitation and restoring	Heave	Examine heave-to-heave PR

also incorporate a viscous damping term, based on the Morison equation [127]. [126]'s model effectively captures PR in various spar-type WECs, including the CorPower [108], Wavebob [109], and OWC Spar Buoy [110,113,128,129].

3.4.5. Computational fluid dynamics

Over 200 WEC-related CFD studies, from 2004–2017, are reviewed in [13], none of which report PR, which is possibly due to the historically feasible CFD simulation run times not surpassing the number of wave periods necessary for the onset of PR. However, later in 2018, [38] noted the occurrence of PR in their CFD studies on a moored HPA, prompting further research on parametric excitation in 6 DoF WECs [111], albeit with a significant computational cost of 1600 CPU hours per wave period. [119,120] used CFD, alongside NLFK simulations, to validate their efficient PR-focused models, which are about an order of magnitude faster than the NLFK model and almost five orders of magnitude faster than the CFD simulations.

3.4.6. Mooring system

Moorings can influence PR in floating WECs. Various mooring models exist, with increasing levels of complexity required for different applications [130]. For taut-moored WECs, which can act like inverted pendulums, [27] utilize a buoyancy pendulum equation to predict sea states likely to induce PR. In [36,106] the mooring tether length varies with the PTO stroke. [36] derive an equation accounting for tether length variation and cast it into the form of the Mathieu equation by assuming sinusoidal heave, then determine stability curves using a shipping method [131]. [106] extends this analysis to include linear hydrodynamics and wave excitation. [107] then applies this model to analyze PR in yaw DoF for a WEC with three mooring tethers and PTOs. For non-taut moorings, [46] examines the potential of the mooring system to counteract PR using a lumped mass mooring model [132]. [113,133] study how mooring line parameters might induce PR in the Spar-buoy OWC, integrating an NLFK model with a quasi-static mooring model.

3.4.7. Comparative analysis of PR modeling approaches

Table 7 synthesizes the key aspects of the different modeling approaches:

Model Fidelity vs. Run Time: Computational efficiency varies significantly across approaches. Time-varying coefficient models (restoring, inertia and excitation) are fastest, with runtimes of order seconds. NLFK models require minutes to hours, while CFD simulations demand days to weeks. This computational hierarchy inversely correlates with the model fidelity.

Analytical vs. Numerical: A key advantage of time-varying coefficient models is their analytical structure, which contrasts with the numerical approaches of NLFK and CFD. Analytical formulations provide deeper physical insight by explicitly relating system behavior to parameter values. Additionally, these models can leverage powerful analysis methods from the field of Nonlinear Dynamics (discussed in Section 5.3), enabling a more systematic understanding of PR mechanisms.

Model Suitability and Performance Trade-offs: Each approach offers unique advantages:

- Time-varying co-efficient models excel at early-stage design and controller development.
- NLFK models provide an optimal balance between accuracy and speed for most applications.
- CFD serves primarily as a validation tool and for understanding complex flow phenomena.
- Mooring models are essential for specific WEC types, but may be unnecessary for others.

Table 7
Comparative analysis of PR modeling approaches for WECs.

Model type	Computational cost	Accuracy	Physical insight	Implementation complexity
Time-varying restoring	Low	Moderate	High	Low
Time-varying inertia	Low	Moderate	High	Medium
Time-varying excitation	Low	Moderate	High	Medium
NLFK forces	Medium	High	Medium	High
CFD	Very high	Very high	Low	Very high
Mooring models	Low-medium	Moderate-high	Medium	Medium-high

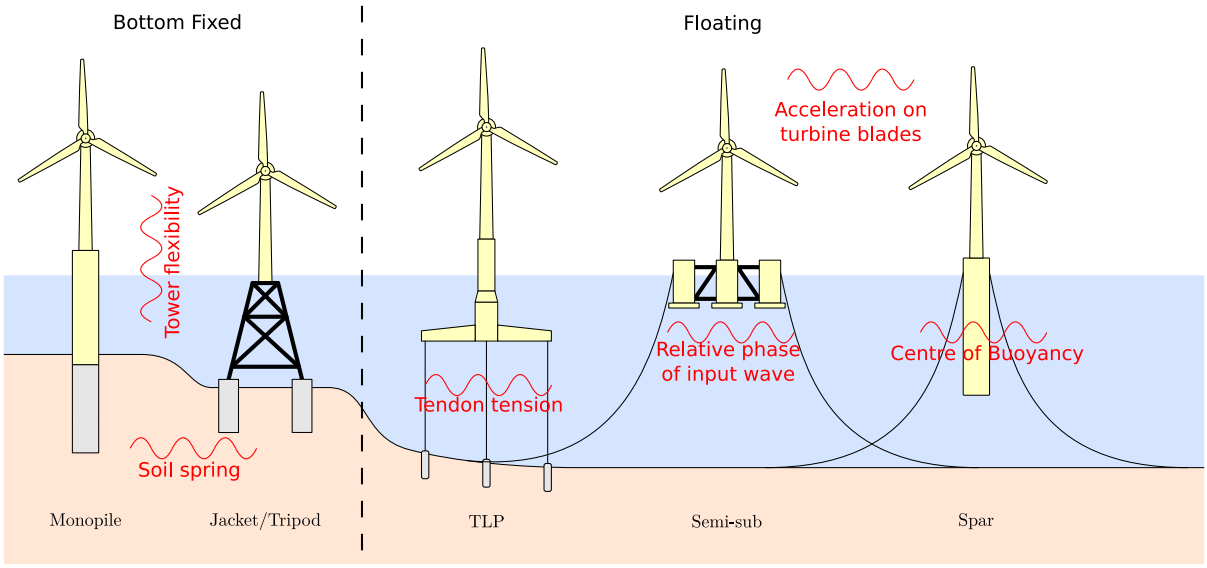

Fig. 9. Types of offshore wind turbines (black) and the main reported driver of PR (red).

4. Offshore wind

During the last decade, OWTs have shifted from bottom-fixed types in nearshore locations to floating OWTs (FOWTs) in deeper waters [134,135], as illustrated in Fig. 9. However, operating on a floating structure makes OWTs more vulnerable to PR. In this section, contrasts are drawn between FOWTs and fixed-bottom OWTs, as well as between FOWTs and WECs. Lessons learned from the analogous dynamic instability of negative damping in FOWTs are also discussed, along with emerging research trends and critical knowledge gaps.

4.1. Bottom fixed vs. floating

Only three studies are found relating to PR in bottom fixed OWTs, summarized in Table 8. PR in bottom-fixed OWTs typically manifests as tower vibrations, dependent on factors such as tower eigenmodes [136] and the soil–structure interaction at the foundation [137]. In contrast, since FOWTs are susceptible to the same PR mechanisms typical of floating structures, a much larger number of studies relate to PR in FOWTs, as summarized in Table 9. The occurrence of PR in a FOWT would result in large-amplitude, unstable motions of the floating structure during certain sea conditions. In addition to affecting normal power production, these unstable motions jeopardize the safety of the FOWT and increase the maximum loading on system components, such as the turbine blades and moorings. Indeed, PR is observed in the turbine blades themselves due to the oscillations of the floating support structure [138].

4.2. FOWT platforms

The three main types of FOWT platforms are depicted in Fig. 9 and compared in Table 10.

4.3. Comparison with WECs

Comparing the amount of literature for WECs and OWTs, highlights a larger prevalence of PR within the context of wave energy. WECs typically aim to maximize wave induced motions, in order to maximize power capture. Whereas, OWTs are designed with the goal of minimizing platform motions, to provide a steady base for the wind turbines. The larger amplitude oscillations of WECs make them more susceptible to PR. However, PR in FOWTs is more difficult to analyze due to the additional forcing from the wind. Considering wind loads on an offshore spar platform is shown to increase the motion amplitudes and influence the occurrence of PR [159].

4.4. Negative damping in FOWT

Negative damping is a dynamic instability unique to FOWTs. If a FOWT employs control methods standard for fixed base wind turbines, the natural periodic motion of the floating platform can be excited from the coupling between the aerodynamic thrust of the turbine and the platform's pitch motion. Lessons from this instability are pertinent for the area of PR. [160] demonstrate that due to the large amplitude motions, a higher fidelity hydrodynamic model (NLFK) is necessary when investigating negative damping and designing FOWT controllers. [161] reveal the presence of bifurcation (discussed in Section 5.3) . Several studies design controllers to avoid negative damping, resulting in trade-offs between the stabilizing the platform motion and parameters such as the blade pitch activity [162], torque demand smoothness [163], power production quality [164] and transient loads suffered by mechanical components [165].

Table 8
Review of publications investigating PR in bottom fixed OWTs.

Ref.	Instability	Focus of paper
[139]	Hydrodynamic field	Occurrence of PR when wave frequency nearly doubles the vortex shedding frequency from masts in steady currents. Leads to heightened velocity fluctuations around the mast, influencing mast design and seabed erosion.
[137]	Tower vibration	Soil–structure interaction influence on PR. Sand compactness influences OWT's natural frequencies and PR identified in loosely packed sands.
[136]	Tower vibration	Mitigate PR with nonlinear proportional derivative controller.

Table 9
Review of publications investigating the existence of PR in FOWTs.

Ref.	Type	Input	Instability	Focus of paper
[140]	Spar with mooring	Regular waves	Pitch	Derivation and validation of stability diagram from Mathieu-type equation
[141,142]	Taut moored spar	Regular waves	Pitch	Experiments and theoretical analyses
[143]	Semi-sub with mooring	Regular waves	Surge	Demonstrating the effect of the structure motion relative to the wave propagation has on the phase of the wave loading
[144,145]	Spar	Regular waves	Pitch	Investigation of combination resonances from heave and pitch coupling
[146]	Combined wind and WEC device, spar with mooring	Regular waves	Pitch	Analysis of survival mode. PR was observed in experiments and subsequent models developed to handle this
[138]	Turbine blades	Regular waves and wind	Turbine Blades	PR in the turbine blades due to the vertical wave excitation
[147]	Spar with mooring and turbine	Irregular waves, wind and current	Pitch	PR due the interaction of wind, wave and VIV loading.
[148–151]	Suction stabilized semi-sub	Regular waves	Pitch/Roll	Analyzing the performance of the Suction Stabilization Method to mitigate PR
[152]	Generic FOWT	Regular waves	Tower vibration	Modeling the FOWT as a cantilever beam with a tip mass and base excitation
[153]	Spar	Regular waves	Pitch	Efficient method to determine PR region
[154]	TLP and Spar with mooring	Regular waves and wind	Pitch	Nonlinear analysis of system dynamics

Table 10
Comparative analysis of PR in different FOWT platforms.

Type	PR risk	DoFs	Key characteristics	Mitigation strategies
Spar	Highest	Mainly pitch, some roll, yaw possible	Small water-plane area and deep draft design amplifies heave–pitch coupling, requiring careful natural frequency tuning	Heave motion reduction, damping fins/heave plates, Natural frequency management
Semi-sub	Medium	Roll, pitch, some surge	Multi-column geometry and bracings introduce complex wave–structure interactions [155]. Wide water-plane area provides inherent stability but also introduces wave-phase differences that trigger PR, like in shipping [118].	Suction Stabilization Method [148–151], Mooring system design [156], increased damping [155].
TLP	Lowest	Sway, surge, some pitch, roll and yaw	Taut moorings reduce vertical motion, decreasing, though not eliminating [154], PR in pitch and roll. However, taut-moorings introduce susceptibility to PR in lateral DoFs [157,158]	Active tension control

5. Lessons from other areas

MRE fields like wave energy and offshore wind are relatively new, therefore valuable insights can be drawn from established disciplines.

5.1. Energy harvesting

Vibration energy harvesting traditionally employs a mass–spring–damper tuned to the dominant vibration frequency. Nonlinear mechanisms to broaden frequency bandwidth, increase power output, and improve response to irregular vibrations are explored [166]. PR is recognized for enhancing power density and expanding frequency range, acting as a mechanical amplifier [167,168]. Jia and Seshia [169] note that driving acceleration must surpass a damping-dependent threshold amplitude to activate this process, prompting research into methods to reduce this threshold [170,171].

To power underwater oceanographic devices, [172,173] adapt a horizontal pendulum concept with a 2:1 pitch-to-roll natural frequency ratio [79] to harness energy from currents using vortex-induced vibrations and PR. [174] investigate enhancing a piezoelectric energy

Table 11
Summary of relevant studies in other offshore fields.

Spars		
Modeling and analysis	Analyzing PR using the hong spar [121] Benchmark test case	[51,123,176–185]
	Effect of moorings Nonlinear dynamics analysis	[186–188] [189]
	The role of wave pressure field in inducing PR	[183,190–192]
Suppression of PR	Fins/strakes Hull design Dynamic vibration absorber	[50,193] [194–196] [185]
Shipping		
Simplified models	1-DOF models use the Mathieu equation to analyze roll motion's stability, drawing from Floquet theory	[118,197,198]
	1.5-DOF models link roll motion to vertical movements (heave/pitch) through hydrostatic calculations of the righting lever	[199–203]
	3-DOF models, where heave, pitch, and roll are interconnected, with wave forces directly affecting the motion equations	[204–208]
Complex numerical models	These models, which incorporate full ship dynamics across 5 or 6 DOFs, evaluate hull designs for their vulnerability to parametric roll	[91,198,209]
Probabilistic models	Predicting the likelihood and severity of large roll motions using statistical analysis and simulation	[202,203,210–212]
Estimation, prediction and monitoring for early detection	State/parameter estimation Signal processing Statistical change detection Machine learning	[213–215] [216–219] [220–223] [224–228]
Control methods	Detuning of the frequency coupling by means of speed and course change	[229–233]
	Damping of roll oscillations by means of passive or active roll-stabilization devices	[198,217–219,227,228,234–240]
Ship-based cranes		
Modeling and analysis	Time-varying restoring term, Mathieu Equation and stability maps	[241,242]
Control methods	Adjusting the cable length and crane motion using control algorithms	[243–245]
Mooring systems		
Tethered buoys	PR in taut moored buoys, resembling inverted pendulum	[246–248]
PR in the lines, cables, risers, etc.	PR in mooring lines PR in TLP tethers PR in risers and pipelines in offshore oil and gas	[249–252] [253,254] [255–263]
	Umbilicals to sea floor equipment for control signals, data, power etc.	[264]

harvester using a hypothetical spring with time-varying stiffness to trigger PR, increasing power output up to 70%.

5.2. Offshore engineering

The study of PR in other offshore fields is summarized in Table 11 and grouped according to:

Spars – Spar buoys are used for a wide range of offshore applications and feature heavily in the types of WECs and FOWTs that experience PR. Research into PR in spars dates back to Derns' [175] 1972 comprehensive study.

Shipping – The study of PR in floating bodies, naval architecture and offshore engineering originates from the shipping industry. PR on ships has been systematically researched since 1950s.

Ship-based Cranes – Wave-induced motions of ship-based cranes can cause significant load swinging, akin to a parametric pendulum.

Mooring Systems – Mooring systems can contribute to the occurrence of PR in floating bodies. In addition, the mooring lines and cables themselves can be subject to PR.

5.3. Nonlinear dynamics

Parametric excitation has been a mainstream research area in the field of Nonlinear Dynamics, with a wealth of analysis tools and techniques being developed. Here we briefly discuss and review the relevant methods that have been applied to WECs, OWTs and offshore applications.

Coexisting attractors – Considering the Hong Spar [121], Habib et al. [184] show the existence of an extensive bistable region, where stable PR coexists with a regular resonance response. This result has the implication that the identification of the PR region is dependent on the initial conditions. This effect is also noted in some WEC papers where Guo and Ringwood [115] find the occurrence of PR is sensitive to the initial conditions and Giorgi [87] shows a significant difference in the PR region when sweeping with increasing frequencies compared to decreasing frequency.

Bifurcation Analysis – Parametric forcing of a system near a Hopf bifurcation is known to yield a complex bifurcation scenarios including quasi-periodic behavior [265,266]. The review on stability of floating bodies in [267], dedicates a section to the bifurcation perspective.

Bifurcation diagrams are employed to evaluate the nonlinear dynamical behavior for an OWC [53], parametric pendulum-type WECs [54,55,59–61,268,269] and the Hong spar [179]. Considering the dynamic characteristics of a rectangular, liquid-filled vessel described by a nonlinear Mathieu-type equation, [270] employ bifurcation diagrams to demonstrate the co-existence of several equilibrium configurations.

Nonlinear normal modes – The application of nonlinear normal modes to analyze the nonlinear and coupled dynamics of an offshore platform is shown in [271]. Nonlinear normal modes are used by Gavassoni et al. to study the parametric instability of the Hong Spar [178] and an offshore tower [272]. Lopes [251] employ nonlinear normal modes for investigation of PR in immersed cables and umbilicals, noting WECs and FOWTs as applications.

Floquet Theory – Floquet theory provides analytical tools for studying stability properties of periodic solutions. It is applied for PR analysis for the case of WECs [52,53], spars [153,154,178], semisubmerisble platforms [151,156], risers and cables [273] and ship based cranes [245].

Method of Multiple Scales – Expresses the system's equations of motion in terms of "slow" and "fast" variables, enabling the dynamics to be analyzed over different time scales to uncover resonance phenomena. This method is applied to examine PR in WECs [56,107], FOWTs [154], Spars [176,180–182] and ship based cranes [243].

Dynamic stability – Wang and Falzarno [274,275] employ various nonlinear dynamics techniques to evaluate the stability of WECs efficiently, highlighting that while classification societies regulate the static stability of large floating structures, their dynamic stability often receives less attention. In addressing irregular wave scenarios, they quantify dynamic stability and the risk of capsizing using stochastic averaging [274] and Melnikov function and Markov process models [275].

Multi-body systems – Ding et al. [276] investigate the existence of PR between the heave and roll DoFs for multi-module floating structures, which could have relevance for multi-body attenuator WECs, such as hinged rafts. Considering the effects of the wave conditions, connector stiffness and number of modules, Ding et al. find that adjusting the connector stiffness could eliminate the PR.

6. Discussion

The discussion first considers four major questions:

- How to identify PR.
- How to reduce PR.
- How to model PR.
- How to assess the impact of PR.

6.1. Identifying parametric resonance

Compared to the case of structural resonance, identifying PR is complicated by an amplitude dependence as well as a frequency dependence, depicted in Fig. 10(a)–(b). While structural resonance can be described by the resonant frequency and the bandwidth, the amplitude dependence of PR requires a region to be identified in the frequency-amplitude space, illustrated in Fig. 10(c)–(d).

There are two main approaches to identifying PR:

- Data-based: These rely on analyzing measured time-series data of relevant DoFs. A common approach is to perform spectral analysis using FFT. Under regular wave conditions, PR is indicated by a noticeable shift in the peak response frequency to around half of the excitation frequency. However, in irregular seas, where input spectra are broad, this method becomes less definitive. Other methods for real-time monitoring of PR in Shipping, listed in Table 11, have been shown to work well in irregular waves, such as the method employed in [51] that monitors the system's instantaneous stability via the eigenvalues of an adaptive dynamic model employing online system identification.
- Analytical: These involve developing reduced-order or analytical models of the system, incorporating time-varying coefficients that capture the periodic variation in key parameters. Tools like Floquet theory and perturbation methods are then used to delineate the boundaries of the PR region.

An additional challenge in identifying PR is the sensitivity to initial conditions. The existence of coexisting attractors, as discussed in Section 5.3, means that the observed PR region can depend significantly on the system's initial state. To mitigate this issue, frequency-sweeping techniques — both upward and downward — are employed to robustly map out the PR region [184]. Moreover, it is essential to ensure that a small but representative amount of energy is initially present in all DoFs, as dynamic coupling may not arise between DoFs if one of them is in the zero state [49,123].

Knowledge Gaps

- Identification Under Irregular Wave Conditions: The build-up of PR typically requires several cycles of excitation at the appropriate frequency and amplitude range. The marine environment is inherently irregular, however most studies employ regular waves to investigate PR, particularly analytical methods which implicitly assume regular wave conditions. The occurrence of PR in multi-frequency irregular wave conditions are less frequently explored and a standard method for identifying PR in irregular waves is currently lacking.
- Routine for Assessing PR Susceptibility in Design: Beyond detection, there is a need for a comprehensive, standardized test routine or protocol that can predict the likelihood of PR occurring in a given design (whether WEC, FOWT, or hybrid systems).
- Impact of Initial Conditions: The dependence of PR on the system's initial state: Systematic studies are needed to quantify how initial energy distributions affect the onset and evolution of PR. Establishing guidelines for setting up experiments or simulations (e.g., minimum initial perturbations across DoFs) would help standardize testing and improve the reproducibility of PR identification.

6.2. Reducing parametric resonance

The most common cause of PR in MRE systems is the periodic variation of the center of buoyancy, which pumps energy into the pitch and roll DoFs. Wave induced motions result in evolving wetted surfaces, which vary the center of buoyancy position. Therefore, an effective strategy to mitigate PR is to reduce the overall wave-induced motion of the body. This strategy works well for FOWTs, where PR suppression techniques developed for generic spars, semi-submersibles and TLPs, that aim to minimize platform motions, can be directly applied. However for WECs, this strategy does not align with the operating principle of large wave-induced motions for energy capture. Therefore, rather than simply suppressing motion, the goal for WECs is to decouple or shift the pitch and roll resonant frequencies away from the frequency range that contributes to power production. This can be achieved either through careful design or through adaptive control strategies that dynamically dampen or decouple energy transfer between DoFs when critical frequencies are approached.

Suppression techniques used in shipping, such as adjusting a vessel's travel speed, are not applicable to stationary MRE devices. However, approaches developed for early detection and prediction of PR in shipping (listed in Table 11) may still be valuable, serving as early-warning indicators for triggering adaptive control measures.

Knowledge Gaps –

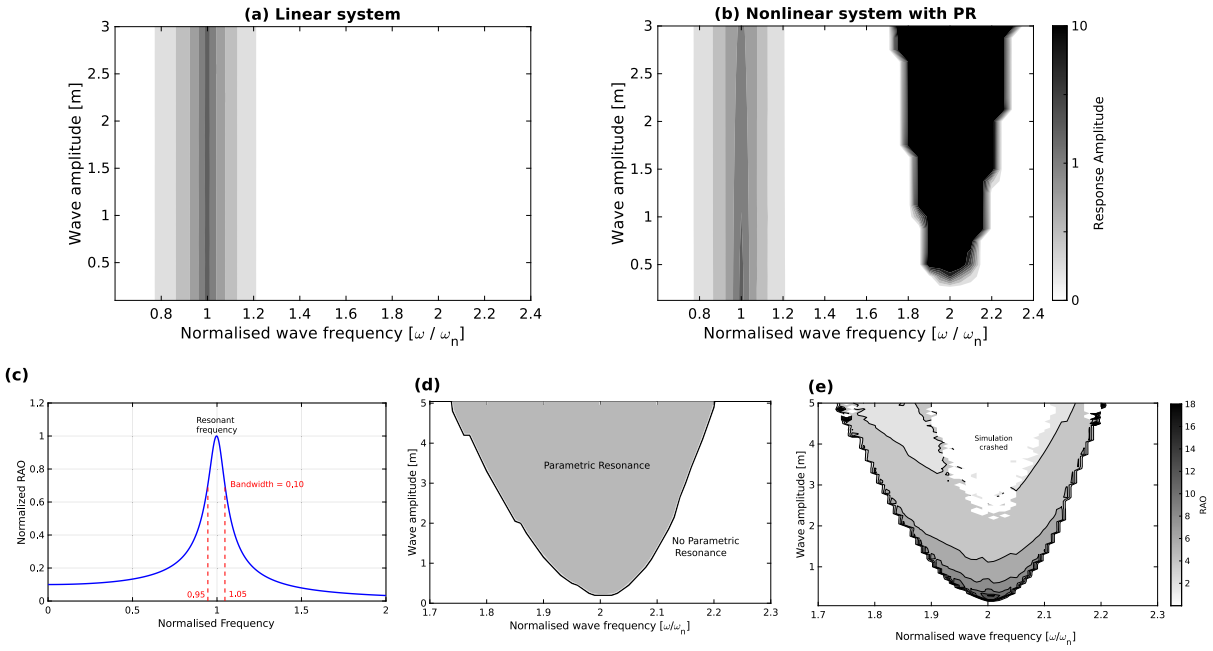

Fig. 10. (a) The result of structural resonance for a linear system in regular waves is a peak in the response amplitude at the natural frequency, with no dependence on the input wave amplitude. (b) For a nonlinear system with PR, the occurrence of large responses around twice the natural frequency are dependent on the input wave amplitude. (c) Description of structural resonance by the resonant frequency and bandwidth. (d) Binary identification of the PR/stability region over the input wave frequency and amplitude space. (e) The parametric amplification domain, proposed by [191], that includes the magnitude of the response for points within the PR region.

- Quantification Under Realistic Conditions: Many suppression techniques have been demonstrated under idealized, regular-wave conditions. Future research should focus on quantifying the cost–benefit and effectiveness of these methods under realistic, irregular sea states, including the potential trade-offs between motion suppression and energy capture.
- Adaptive Control Strategies: There is a need for robust, adaptive control systems that can dynamically mitigate PR without compromising the primary energy capture in WECs or the operational stability of FOWTs. Further work is required to integrate real-time monitoring with control algorithms that can effectively decouple or dampen critical modes of motion.
- Multi-Objective Design Frameworks: For WECs, the inherent conflict between maximizing wave-induced motion for power production and minimizing PR-induced instabilities calls for multi-objective design frameworks. These frameworks should balance energy capture, structural integrity, and long-term reliability.

6.3. Modeling parametric resonance

A range of modeling approaches have been developed, each offering distinct advantages and trade-offs in computational cost, accuracy, and applicability. This diversity in methods, as mapped in Fig. 11, showcases their complementary roles: from initial design exploration with analytical models to detailed validation with CFD, and comprehensive system analysis with hybrids.

Knowledge Gaps –

- Full 6-DoF Validation: Unintended couplings between DoFs can emerge, particularly due to mooring systems, thus validating stability across all 6-DoFs is important to avoid oversight of instabilities like yaw or surge.
- Probabilistic Modeling: The absence of probabilistic models in MRE literature, despite their use in offshore fields (e.g., [203, 210,255]), limits uncertainty quantification for PR likelihood and severity due to environmental and structural variability.
- Benchmark Verification and Validation: Standardized benchmark cases are lacking to quantitatively compare modeling approaches, hindering clear guidelines for method selection.
- Hybrid Methods: Improving the accuracy of lower fidelity models by identifying terms and parameters from the outputs of higher fidelity models (e.g. add a viscous damping term to NLFK models and tune the parameters based on data from CFD experiments). Such Hybrid Methods show promise, but their standardization and widespread adoption require further development.
- Long-Term Impacts: Current models focus on PR onset and amplitude, neglecting its prolonged effects on fatigue life and system reliability. Time-domain simulations integrating fatigue analysis are needed to assess operational durability.

6.4. Assessing parametric resonance

Assessing the impact of PR in MRE systems has typically focused on quantifying the effect on the power output, yet its broader implications span structural fatigue, device safety, and economic impacts across the MRE lifecycle — from design to maintenance. For example, Patel et al. [277] developed a cost estimation model for downtime in offloading operations due to parametric roll, highlighting its economic impact — a lesson directly applicable to MRE installation and maintenance logistics. Fig. 12 structures the assessment of PR throughout the different stages of the MRE device life-cycle.

Knowledge Gaps –

- Reliability Assessment – PR may accelerate material fatigue and lead to premature failure of components. A comprehensive reliability assessment framework, incorporating fatigue analysis and probabilistic modeling, is necessary to evaluate the long-term impacts of PR on MRE systems. For example, [248] present a methodology for assessing instability in mooring systems, providing a useful reference for PR in MRE systems.
- Uncertainty Analysis – Incorporating uncertainty analysis into the study of PR is crucial for robust and resilient MRE system design, however such studies are lacking in the reviewed literature for

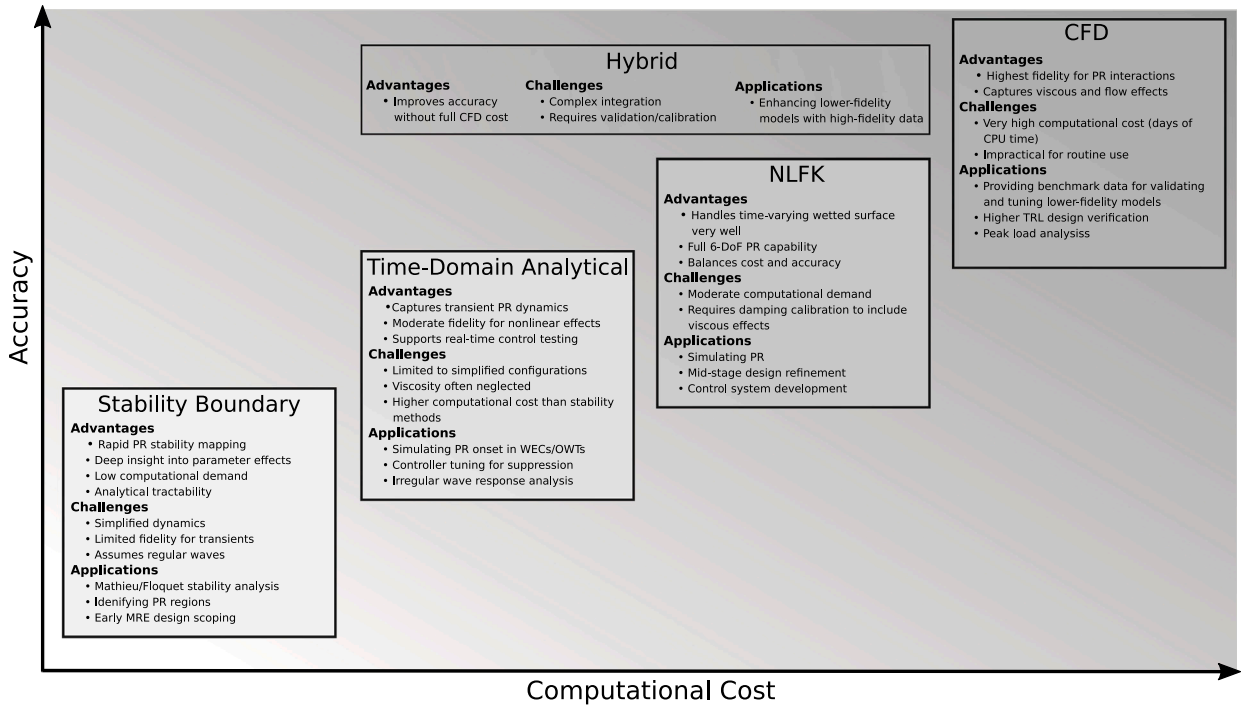

Fig. 11. Comparative overview of modeling approaches for PR in MRE systems.

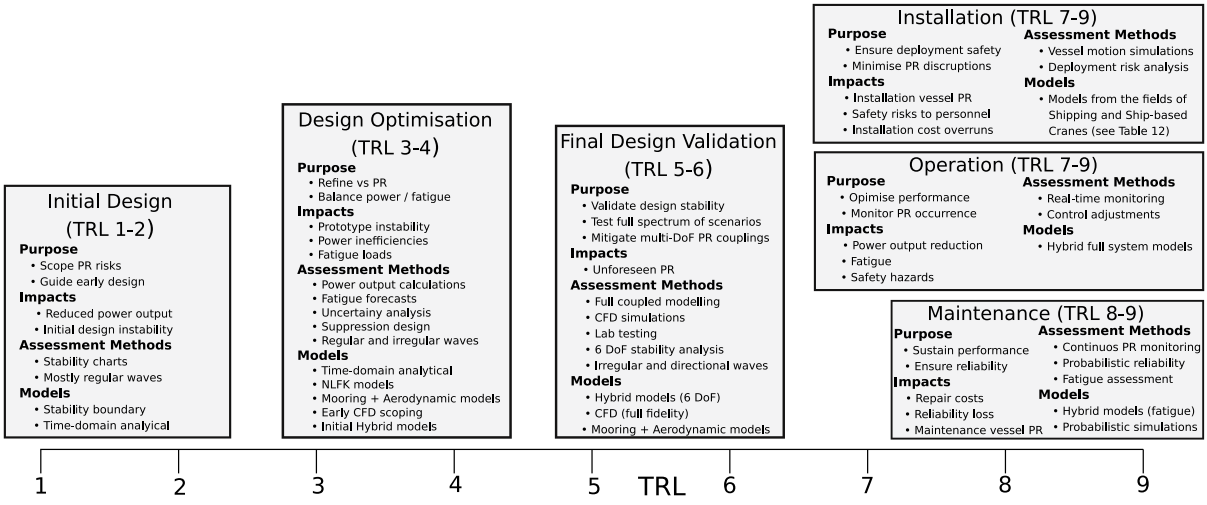

Fig. 12. Assessing PR across MRE TRL stages.

MRE systems. Factors such as varying environmental conditions, material properties, and structural responses can significantly influence the occurrence and impact of PR. For example, [255] adopt a probabilistic approach to evaluate the instability of a top tension riser under irregular sea conditions, accounting for uncertainties in load, structural geometry, and material properties. Applying similar methodologies to WECs and FOWTs can provide a deeper understanding of PR dynamics and improve system reliability.

7. Conclusions

PR is a dynamic instability that can affect MRE devices. In the case of WECs, the occurrence of PR may significantly reduce the energy harvesting and increase structural, mooring and fatigue problems. Analogously, the appearance of PR in FOWTs may have severe negative impacts on the power output and structural health. These negative effects highlight the importance of understanding the nonlinear dynamics of these MRE systems in order to mitigate the occurrence of PR.

Promising solutions to dampen PR have emerged, ranging from passive design optimizations to active control strategies that adjust system dynamics. Yet, their effectiveness must be balanced against operational demands, particularly for WECs where energy capture is paramount. Several research avenues require further exploration:

(i) Developing advanced control techniques to mitigate PR under diverse sea conditions, incorporating real-time monitoring for adaptive responses.

(ii) Exploiting PR to enhance WEC energy conversion, turning its instability into an asset for improved performance.
(iii) Integrating FOWT platforms with WECs to attenuate PR, leveraging coupled dynamics for stability, in addition to increased energy harvesting.
(iv) Assessing PR's long-term effects on reliability and fatigue life, using probabilistic and uncertainty analyses to bolster system resilience.

The review emphasizes the need for a multifaceted approach to address PR in MRE systems, integrating advanced modeling techniques, reliability assessments, and control strategies. By learning from related fields and incorporating comprehensive risk assessments, the development of MRE technologies can advance towards more reliable, efficient, and resilient solutions.

Declaration of generative AI and AI-assisted technologies in the writing process

During the preparation of this work the authors used Claude in order to reduce the word count by rewriting selected paragraphs more concisely. After using this tool/service, the authors reviewed and edited the content as needed and take full responsibility for the content of the publication.

Declaration of competing interest

The authors declare that they have no known competing financial interests or personal relationships that could have appeared to influence the work reported in this paper.

Acknowledgments

Josh Davidson is funded by MCIN and by the European Union NextGenerationEU/PRTR-C17.I1, as well as by IKUR Strategy under the collaboration agreement between Ikerbasque Foundation and BCAM on behalf of the Department of Education of the Basque Government.

João Henriques was partially funded by the Portuguese Foundation for Science and Technology (FCT), through IDMEC, under LAETA project UID/EMS/50022/2020.

This work has been supported by the Hungarian National Research, Development and Innovation Fund under contracts NKFI K 137726 and K137699. The research reported in this paper is part of project no. TKP-6-6/PALY-2021. Project no. TKP-6-6/PALY-2021 has been implemented with the support provided by the Ministry of Culture and Innovation of Hungary from the National Research, Development and Innovation Fund, financed under the TKP2021-NVA funding scheme.

Data availability

Data will be made available on request.

References

[1] Faraday M. On a peculiar class of acoustical figures; and on certain forms assumed by groups of particles upon vibrating elastic surfaces. Philos Trans R Soc Lond 1831;121:299–340. http://dx.doi.org/10.1098/rspl.1830.0024.
[2] Melde F. Ueber die Erregung stehender Wellen eines fadenförmigen Körpers. Ann Phys, Lpz 1860;185(2):193– 215. http://dx.doi.org/10.1002/andp.18601850202.
[3] Mathieu E. Mémoire sur le mouvement vibratoire d'une membrane de forme elliptique. J Math Pures Appl 1868;13:137–203.
[4] Cunningham WJ. Introduction to nonlinear analysis. McGraw-Hill electrical and electronic engineering series, McGraw-Hill; 1958.
[5] Bolotin VV. The dynamic stability of elastic systems. Series in mathematical physics, Holden-Day; 1964.
[6] Tondl A, Ruijgrok T, Verhulst F, Nabergoj R. Autoparametric resonance in mechanical systems. Cambridge University Press; 2000.
[7] Butikov EI. Simulations of oscillatory systems: with award-winning software, physics of oscillations. CRC Press; 2015, http://dx.doi.org/10.1201/b18110.
[8] Champneys A. Dynamics of parametric excitation. In: Meyers RA, editor. Mathematics of complexity and dynamical systems. New York, NY: Springer New York; 2011, p. 183–204. http://dx.doi.org/10.1007/978-1-4614-1806-1_13.
[9] Pedersen P. On stability diagrams for damped Hill equations. Quart Appl Math 1985;42(4):477–95. http://dx.doi.org/10.1090/qam/766884.
[10] Froude W. Remarks on Mr. Scott Russel's paper on rolling. Trans Inst Nav Archit 1863;4:232–75.
[11] Froude W. On the rolling of ships. Trans Inst Nav Archit 1861;2(9):180–227.
[12] Thornton ST, Marion JB. Classical dynamics of particles and systems. Cengage Learning; 2004.
[13] Windt C, Davidson J, Ringwood JV. High-fidelity numerical modelling of ocean wave energy systems: A review of computational fluid dynamics-based numerical wave tanks. Renew Sustain Energy Rev 2018;93:610–30. http://dx.doi.org/10.1016/j.rser.2018.05.020.
[14] WAMIT. 2023, https://www.wamit.com/. Online, [Accessed 11 2023].
[15] Ansys AQWA. 2023, https://www.ansys.com/products/structures/ansys-aqwa. Online, [Accessed 11 2023].
[16] Nemoh. 2023, https://lheea.ec-nantes.fr/valorisation/logiciels-et-brevets/nemoh-presentation. Online, [Accessed 11 2023].
[17] Capytaine. 2023, https://capytaine.org/. Online, [Accessed 11 2023].
[18] HAMS. 2023, https://github.com/YingyiLiu/HAMS. Online, [Accessed 11 2023].
[19] Zabala I, Henriques JCC, Kelly TE, Ricci PP, Blanco JM. Post-processing techniques to improve the results of hydrodynamic boundary element method solvers. Ocean Eng 2024;295:116913. http://dx.doi.org/10.1016/j.oceaneng.2024.116913.
[20] Davidson J, Henriques JCC, Gomes RPF, Galeazzi R. Opening the air-chamber of an oscillating water column spar buoy wave energy converter to avoid parametric resonance. IET Renew Power Gener 2021;15(14):3109–25. http://dx.doi.org/10.1049/rpg2.12204.
[21] Davidson J, Henriques JCC. OWC spar bouy - parametric pitch and roll motion. 2022, https://www.youtube.com/@nonlinearrockandroll8690. Online, [Accessed 04 2024].
[22] Bracewell RH. Frog and PS frog: a study of two reactionless ocean wave energy converters (Ph.D. thesis), University of Lancaster; 1990.
[23] Wavegen. Research into the further development of the LIMPET shoreline wave energy plant. Tech. rep., DTI Sustainable EnergyProgramme; 2002, V/06/00183/00/Rep.
[24] Durand M, Babarit A, Pettinotti B, Quillard O, Toularastel J, Clément A. Experimental validation of the performances of the SEAREV wave energy converter with real time latching control. In: EWTEC 2007, 7th European wave and tidal energy conference, Porto, Portugal. 2007, p. 1–6.
[25] Payne GS, Taylor JRM, Bruce T, Parkin P. Assessment of boundary-element method for modelling a free-floating sloped wave energy device. Part 2: Experimental validation. Ocean Eng 2008;35(3–4):342–57. http://dx.doi.org/10.1016/j.oceaneng.2007.10.008.
[26] Raftery MW. Harnessing ocean surface wave energy to generate electricity (Master's thesis), Stevens Institute of Technology; 2008.
[27] Nicoll RS, Wood CF. Nonlinear parametric analysis of a wave energy converter. In: Proceedings of the 2010 CSME forum, Victoria, British Columbia. 2010.
[28] Weller S, Stallard T, Stansby P. Two-dimensional motions of a shallow draft wave energy converter undergoing regular wave excitation. In: EWTEC 2011, 9th European wave and tidal energy conference, Southampton, UK. 2011.
[29] Sheng W, Flannery B, Lewis A, Alcorn R. Experimental studies of a floating cylindrical OWC WEC. In: ASME 2012, 31st international conference on ocean, offshore and arctic engineering. 2012, http://dx.doi.org/10.1115/OMAE2012-83040.
[30] Gomes RPF, Henriques JCC, Gato LMC, Falcao AFO. Testing of a small-scale floating OWC model in a wave flume. In: International conference on ocean energy. 2012, p. 1–7.
[31] Gomes RPF, Henriques JCC, Gato LMC, Falcão AFO. Wave channel tests of a slack-moored floating oscillating water column in regular waves. In: EWTEC 2015, 11th European wave and tidal energy conference, Nantes, France. 2015, p. 6–11.
[32] Fonseca F-XCD, Gomes RPF, Henriques JCC, Gato LMC, Falcão AFO. Model testing of an oscillating water column spar-buoy wave energy converter isolated and in array: Motions and mooring forces. Energy 2016;112:1207–18. http://dx.doi.org/10.1016/j.energy.2016.07.007.
[33] Gomes RPF, Henriques JCC, Gato LMC, Falcão AFO. Experimental tests of a 1:16th-scale model of the spar-buoy OWC in a large scale wave flume in regular waves. In: ASME 2018, 37th international conference on ocean, offshore and arctic engineering. American Society of Mechanical Engineers Digital Collection; 2018.
[34] Gomes RPF, Henriques JCC, Gato LMC, Falcão AFO. Time-domain simulation of a slack-moored floating oscillating water column and validation with physical model tests. Renew Energy 2020;149:165–80. http://dx.doi.org/10.1016/j.renene.2019.11.159.

[35] Beatty SJ, Roy A, Bubbar K, Ortiz J, Buckham BJ, Wild P, Stienke D, Nicoll R. Experimental and numerical simulations of moored self-reacting point absorber wave energy converters. In: 25th international ocean and polar engineering conference. 2015.

[36] Orszaghova J, Wolgamot H, Taylor RE, Draper S, Rafiee A, Taylor PH. Simplified dynamics of a moored submerged buoy. In: 32nd international workshop on water waves and floating bodies, Dalian, China. 2017.

[37] Sergiienko NY. Three-tether wave energy converter: hydrodynamic modelling, performance assessment and control (Ph.D. thesis), University of Adelaide; 2018.

[38] Eskilsson C, Palm J, Bergdahl L. Simulations of Moored wave energy converters using openFOAM: Implementation and applications. In: 6th world maritime technology conference. 2018.

[39] Kurniawan A, Grassow M, Ferri F. Numerical modelling and wave tank testing of a self-reacting two-body wave energy device. Ships Offshore Struct 2019;14(sup1):1–13. http://dx.doi.org/10.1080/17445302.2019.1595924.

[40] Wang H, Somayajula A, Falzarano J, Xie Z. Development of a blended time-domain program for predicting the motions of a wave energy structure. J Mar Sci Eng 2020;8(1):1. http://dx.doi.org/10.3390/jmse8010001.

[41] Giassi M, Thomas S, Tosdevin T, Engström J, Hann M, Isberg J, Göteman M. Capturing the experimental behaviour of a point-absorber WEC by simplified numerical models. J Fluids Struct 2020;99:103143. http://dx.doi.org/10.1016/j.jfluidstructs.2020.103143.

[42] Giassi M, Engström J, Isberg J, Göteman M. Comparison of wave energy park layouts by experimental and numerical methods. J Mar Sci Eng 2020;8(10):750. http://dx.doi.org/10.3390/jmse8100750.

[43] Giassi M. Numerical and experimental modelling for wave energy arrays optimization (Ph.D. thesis), Uppsala University; 2020.

[44] Villegas C, Schaaf HVD. Implementation of a pitch stability control for a wave energy converter. In: EWTEC 2011, 10th European wave and tidal energy conference, Southampton, UK. 2011.

[45] Cordonnier J, Gorintin F, Cagny AD, Clément AH, Babarit A. SEAREV: Case study of the development of a wave energy converter. Renew Energy 2015;80:40–52. http://dx.doi.org/10.1016/j.renene.2015.01.061.

[46] Ortiz JP. The influence of mooring dynamics on the performance of self reacting point absorbers (Master's thesis), University of Victoria; 2016.

[47] Gomes RPF, Ferreira JM, Ribeiro e Silva S, Henriques JCC, Gato LMC. An experimental study on the reduction of the dynamic instability in the oscillating water column spar buoy. In: EWTEC 2017, 12th European wave and tidal energy conference, Cork, UK. 2017.

[48] Gomes RPF, Henriques JCC, Gato LMC, Falcao AFO. An upgraded model for the design of spar-type floating oscillating water column devices. In: EWTEC 2019, 13th European wave and tidal energy conference, Naples, Italy. 2019.

[49] Maloney P. Performance assessment of a 3-body self-reacting point absorber type wave energy converter (Master's thesis), University of Victoria; 2019.

[50] Rho JB, Choi HS, Shin HS, Park IK, et al. A study on mathieu-type instability of conventional spar platform in regular waves. Int J Offshore Polar Eng 2005;15(feb):607–15.

[51] Davidson J, Kalmár-Nagy T. A real-time detection system for the onset of parametric resonance in wave energy converters. J Mar Sci Eng 2020;8(10):819. http://dx.doi.org/10.3390/jmse8100819.

[52] Lippmann H. Direct energy conversion from water waves into electromagnetic oscillations. Arch Appl Mech 1995;65(4):279–90. http://dx.doi.org/10.1007/bf00805467.

[53] Olvera A, Prado E, Czitrom S. Parametric resonance in an oscillating water column. J Engrg Math 2007;57(1):1–21. http://dx.doi.org/10.1007/s10665-006-9048-z.

[54] Xu X. Nonlinear dynamics of parametric pendulum for wave energy extraction (Ph.D. thesis), University of Aberdeen; 2005.

[55] Horton BW, Wiercigroch M. Effects of heave excitation on rotations of a pendulum for wave energy extraction. In: IUTAM symposium on fluid-structure interaction in ocean engineering. Springer; 2008, p. 117–28. http://dx.doi.org/10.1007/978-1-4020-8630-4_11.

[56] Horton B. Rotational motion of pendula systems for wave energy extraction (Ph.D. thesis), University of Aberdeen; 2009.

[57] Najdecka A, Vaziri V, Wiercigroch M. Synchronization control of parametric pendulums for wave energy extraction. In: Proceedings of the international conference on renewable energies and power quality. 2010, http://dx.doi.org/10.24084/repqj09.383.

[58] Wiercigroch M, Najdecka A, Vaziri V. Nonlinear dynamics of pendulums system for energy harvesting. In: Vibration problems ICOVP 2011. Springer; 2011, p. 35–42. http://dx.doi.org/10.1007/978-94-007-2069-5_4.

[59] Lenci S, Rega G. Experimental versus theoretical robustness of rotating solutions in a parametrically excited pendulum: a dynamical integrity perspective. Phys D: Nonlinear Phenom 2011;240(9–10):814–24. http://dx.doi.org/10.1016/j.physd.2010.12.014.

[60] Lenci S, Brocchini M, Lorenzoni C. Experimental rotations of a pendulum on water waves. J Comput Nonlinear Dyn 2012;7(1). http://dx.doi.org/10.1115/1.4004547.

[61] Paula ASD, Savi MA, Wiercigroch M, Pavlovskaia E. Bifurcation control of a parametric pendulum. Int J Bifurc Chaos 2012;22(05):1250111. http://dx.doi.org/10.1142/s0218127412501118.

[62] Yurchenko D, Alevras P. Dynamics of the N-pendulum and its application to a wave energy converter concept. Int J Dyn Control 2013;1(4):290–9. http://dx.doi.org/10.1007/s40435-013-0033-x.

[63] Vaziri V, Najdecka A, Wiercigroch M. Experimental control for initiating and maintaining rotation of parametric pendulum. Eur Phys J Spec Top 2014;223(4):795–812. http://dx.doi.org/10.1140/epjst/e2014-02141-y.

[64] Alevras P, Yurchenko D. Stochastic rotational response of a parametric pendulum coupled with an SDOF system. Probab Eng Mech 2014;37:124–31. http://dx.doi.org/10.1016/j.probengmech.2013.10.008.

[65] Alevras P, Yurchenko D, Naess A. Energy response probability density function of a rotating parametric pendulum. In: Vulnerability, uncertainty, and risk. American Society of Civil Engineers; 2014, p. 1866–74. http://dx.doi.org/10.1061/9780784413609.187.

[66] Alevras P, Brown I, Yurchenko D. Experimental investigation of a rotating parametric pendulum. Nonlinear Dynam 2015;81(1–2):201–13. http://dx.doi.org/10.1007/s11071-015-1982-8.

[67] Alevras P. Rotating potential of a stochastic parametric pendulum (Ph.D. thesis), Heriot-Watt University; 2015.

[68] Andreeva T, Alevras P, Naess A, Yurchenko D. Dynamics of a parametric rotating pendulum under a realistic wave profile. Int J Dyn Control 2016;4(2):233–8. http://dx.doi.org/10.1007/s40435-015-0168-z.

[69] Reguera F, Dotti FE, Machado SP. Rotation control of a parametrically excited pendulum by adjusting its length. Mech Res Commun 2016;72:74–80. http://dx.doi.org/10.1016/j.mechrescom.2016.01.011.

[70] Yurchenko D, Alevras P. Parametric pendulum based wave energy converter. Mech Syst Signal Process 2018;99:504–15. http://dx.doi.org/10.1016/j.ymssp.2017.06.026.

[71] Dostal L, Korner K, Kreuzer E, Yurchenko D. Pendulum energy converter excited by random loads. ZAMM- J Appl Math Mech/ Z Angew Math Mech 2018;98(3):349–66. http://dx.doi.org/10.1002/zamm.201700007.

[72] Dostal L, PICK M-A. Theoretical and experimental study of a pendulum excited by random loads. European J Appl Math 2019;30(5):912–27. http://dx.doi.org/10.1017/s0956792518000529.

[73] Orazov B, O'Reilly OM, Savaş Ö. On the dynamics of a novel ocean wave energy converter. J Sound Vib 2010;329(24):5058–69. http://dx.doi.org/10.1016/j.jsv.2010.07.007.

[74] Orazov B. A novel excitation scheme for an ocean wave energy converter (Ph.D. thesis), University of California, Berkeley; 2011.

[75] Orazov B, O'Reilly OM, Zhou X. On forced oscillations of a simple model for a novel wave energy converter. Nonlinear Dynam 2012;67(2):1135–46. http://dx.doi.org/10.1007/s11071-011-0058-7.

[76] Rougirel A. Mathematical analysis of a wave energy converter model. Nonlinear Anal Real World Appl 2013;14(1):434–54. http://dx.doi.org/10.1016/j.nonrwa.2012.07.007.

[77] Diamond CA, O'Reilly OM, Savaş Ö. The impulsive effects of momentum transfer on the dynamics of a novel ocean wave energy converter. J Sound Vib 2013;332(21):5559–65. http://dx.doi.org/10.1016/j.jsv.2013.05.030.

[78] Diamond CA, Judge CQ, Orazov B, Savaş Ö, O'Reilly OM. Mass-modulation schemes for a class of wave energy converters: Experiments, models, and efficacy. Ocean Eng 2015;104:452–68. http://dx.doi.org/10.1016/j.oceaneng.2015.05.018.

[79] Yerrapragada K, Ansari MH, Karami MA. Enhancing power generation of floating wave power generators by utilization of nonlinear roll-pitch coupling. Smart Mater Struct 2017;26(9):094003. http://dx.doi.org/10.1088/1361-665x/aa7710.

[80] Abdelkhalik O, Zou S, Robinett R, Bacelli G, Wilson D, Coe R. Control of three degrees-of-freedom wave energy converters using pseudo-spectral methods. J Dyn Syst Meas Control 2018;140(7):074501. http://dx.doi.org/10.1115/1.4038860.

[81] Zou S, Abdelkhalik O, Robinett R, Korde U, Bacelli G, Wilson D, Coe R. Model predictive control of parametric excited pitch-surge modes in wave energy converters. Int J Mar Energy 2017;19:32–46. http://dx.doi.org/10.1016/j.ijome.2017.05.002.

[82] Zou S, Abdelkhalik O. Time-varying linear quadratic Gaussian optimal control for three-degree-of-freedom wave energy converters. Renew Energy 2020;149:217–25. http://dx.doi.org/10.1016/j.renene.2019.12.054.

[83] Lelkes J, Davidson J, Kalmár-Nagy T. Modelling of parametric resonance for heaving buoys with position-Varying Waterplane Area. J Mar Sci Eng 2021;9(11):1162. http://dx.doi.org/10.3390/jmse9111162.

[84] Ribeiro e Silva S, Gomes RPF, Lopes BS, Carrelhas AAD, Gato LMC, Henriques JCC, Gordo JM, Falcão AFO. Model testing of a floating wave energy converter with an internal U-shaped oscillating water column. Energy Convers Manage 2021;240:114211. http://dx.doi.org/10.1016/j.enconman.2021.114211.

[85] Giorgi G, Faedo N, Mattiazzo G. Time-varying damping coefficient to increase power extraction from a notional wave energy harvester. In: 2021 international conference on electrical, computer, communications and mechatronics engineering. ICECCME, IEEE; 2021, p. 1–6. http://dx.doi.org/10.1109/iceccme52200.2021.9591020.

[86] Jiang X, Shi H, Cao F, Zhao Z, Li M, Chen Z. System analysis and experimental investigation of a pendulum-based wave energy converter. Ocean Eng 2023;277:114300. http://dx.doi.org/10.1016/j.oceaneng.2023.114300.

[87] Giorgi G. Embedding parametric resonance in a 2:1 wave energy converter to get a broader bandwidth. Renew Energy 2024;222:119928. http://dx.doi.org/10.2139/ssrn.4523769.

[88] Giorgi G. The onset of instability in a parametric resonance energy harvester under panchromatic excitations. Int J Mech Sci 2024;281:109544. http://dx.doi.org/10.1016/j.ijmecsci.2024.109544.

[89] Dotti FE, Reguera F, Machado SP. A review on the nonlinear dynamics of pendulum systems for energy harvesting from ocean waves. In: Proceedings of the 1st pan-American congress on computational mechanics. PANACM, 2015, p. 1516–29.

[90] Song Z, Bao Y, Zhang D, Shu Q, Song Y, Qiao F. Centuries of monthly and 3-hourly global ocean wave data for past, present, and future climate research. Sci Data 2020;7(1):226. http://dx.doi.org/10.1038/s41597-020-0566-8.

[91] Ribeiro e Silva S, Santos TA, Guedes Soares C. Parametrically excited roll in regular and irregular head seas. Int Shipbuild Prog 2005;52(1):29–56.

[92] Ribeiro e Silva S, Guedes Soares C. Prediction of parametric rolling in waves with a time domain non-linear strip theory model. Ocean Eng 2013;72:453–69. http://dx.doi.org/10.1016/j.oceaneng.2013.07.011.

[93] Schumacher A, Ribeiro e Silva S, Guedes Soares C. Experimental and numerical study of a containership under parametric rolling conditions in waves. Ocean Eng 2016;124:385–403. http://dx.doi.org/10.1016/j.oceaneng.2016.07.034.

[94] Haslum HA, Faltinsen OM. Alternative shape of spar platforms for use in hostile areas. In: Offshore technology conference, Houston, Texas. 1999, http://dx.doi.org/10.4043/10953-MS.

[95] Haslum HA. Simplified methods applied to nonlinear motion of spar platforms (Ph.D. thesis), Norwegian University of Science and Technology; 2000.

[96] Jang H, Kim M. Mathieu instability of arctic spar by nonlinear time-domain simulations. Ocean Eng 2019;176:31–45. http://dx.doi.org/10.1016/j.oceaneng.2019.02.029.

[97] Jang H, Kim M. Effects of nonlinear FK (Froude-Krylov) and hydrostatic restoring forces on arctic-spar motions in waves. Int J Nav Archit Ocean Eng 2020;12:297–313. http://dx.doi.org/10.1016/j.ijnaoe.2020.01.002.

[98] Billah KY. On the definition of parametric excitation for vibration problems. J Sound Vib 2004;270(1–2):450–4. http://dx.doi.org/10.1016/s0022-460x(03)00408-5.

[99] Scapolan M, Tehrani MG, Bonisoli E. Energy harvesting using parametric resonant system due to time-varying damping. Mech Syst Signal Process 2016;79:149–65. http://dx.doi.org/10.1016/j.ymssp.2016.02.037.

[100] Tehrani MG, Pumhoessel T. Impulsive parametric damping in energy harvesting. J Phys: Conf Ser 2016;744(1):012081. http://dx.doi.org/10.1088/1742-6596/744/1/012081.

[101] Falnes J. Ocean waves and oscillating systems. Cambridge University Press; 2002, http://dx.doi.org/10.1017/cbo9780511754630.

[102] Folley M. Numerical modelling of wave energy converters: state-of-the-art techniques for single devices and arrays. Academic Press; 2016.

[103] Babarit A, Mouslim H, Clément A, Laporte-Weywada P. On the numerical modelling of the nonlinear behaviour of a wave energy converter. In: 28th international conference on offshore mechanics & arctic engineering. 2009.

[104] Tarrant KR. Numerical modelling of parametric resonance of a heaving point absorber wave energy converter (Ph.D. thesis), Trinity College Dublin; 2015.

[105] Tarrant K, Meskell C. Investigation on parametrically excited motions of point absorbers in regular waves. Ocean Eng 2016;111:67–81. http://dx.doi.org/10.1016/j.oceaneng.2015.10.041.

[106] Orszaghova J, Wolgamot H, Draper S, Taylor RE, Taylor PH, Rafiee A. Transverse motion instability of a submerged moored buoy. Proc R Soc A 2019;475(2221):20180459. http://dx.doi.org/10.1098/rspa.2018.0459.

[107] Orszaghova J, Wolgamot H, Draper S, Taylor PH, Rafiee A. Onset and limiting amplitude of yaw instability of a submerged three-tethered buoy. Proc R Soc A 2020;476(2235):20190762. http://dx.doi.org/10.1098/rspa.2019.0762.

[108] Giorgi G, Ringwood JV. A compact 6-DoF nonlinear wave energy device model for power assessment and control investigations. IEEE Trans Sustain Energy 2018;10(1):119–26. http://dx.doi.org/10.1109/tste.2018.2826578.

[109] Giorgi G, Ringwood JV. Articulating parametric nonlinearities in computationally efficient hydrodynamic models. IFAC- Pap 2018;51(29):56–61. http://dx.doi.org/10.1016/j.ifacol.2018.09.469.

[110] Giorgi G, Ringwood JV. Parametric motion detection for an oscillating water column spar buoy. In: Advances in renewable energies offshore - proceedings of the 3rd international conference on renewable energies offshore RENEW 2018, Lisbon, Portugal. CRC Press; 2018, p. 505–12.

[111] Palm J, Bergdahl L, Eskilsson C. Parametric excitation of moored wave energy converters using viscous and non-viscous CFD simulations. In: Advances in renewable energies offshore - proceedings of the 3rd international conference on renewable energies offshore, RENEW 2018, Lisbon, Portugal. CRC Press; 2019, p. 455–62.

[112] Davidson J, Karimov M, Szelechman A, Windt C, Ringwood J. Dynamic mesh motion in openFOAM for wave energy converter simulation. In: 14th openFOAM workshop, Duisburg, Germany. 2019.

[113] Giorgi G, Bracco G, Mattiazzo G, Gomes RPF. Effect of mooring line attachment point on parametrically excited motions and power extraction in the spar-buoy OWC device. In: Developments in renewable energies offshore. Vol. 5, Taylor & Francis; 2020, p. 635–43.

[114] Silva LSP, Sergiienko NY, Pesce CP, Ding B, Cazzolato B, Morishita HM. Stochastic analysis of nonlinear wave energy converters via statistical linearization. Appl Ocean Res 2020;95:102023. http://dx.doi.org/10.1016/j.apor.2019.102023.

[115] Guo B, Ringwood J. On energy transfer of parametric resonance for wave energy conversion. In: EWTEC 2021, 14th European wave and tidal energy conference, Plymouth, UK. 2021.

[116] Guo B, Ringwood JV. Examination of the virtues of parametric energy coupling in wave energy conversion. Int Mar Energy J 2022;5(2):219–26. http://dx.doi.org/10.36688/imej.5.219-226.

[117] Nayfeh AH, Mook DT, Marshall LR. Nonlinear coupling of pitch and roll modes in ship motions. J Hydronaut 1973;7(4):145–52. http://dx.doi.org/10.2514/3.62949.

[118] Kerwin JE. Notes on rolling in longitudinal waves. Int Shipbuild Prog 1955;2(16):597–614. http://dx.doi.org/10.3233/isp-1955-21604.

[119] Kurniawan A, Tran TT, Brown SA, Eskilsson C, Orszaghova J, Greaves D. Numerical simulation of parametric resonance in point absorbers using a simplified model. IET Renew Power Gener 2021;15(14):3186–205. http://dx.doi.org/10.1049/rpg2.12229.

[120] Kurniawan A, Tran TT, Yu Y-H. An efficient time-domain model to simulate parametric resonances in a floating body free to move in six degrees of freedom. In: ASME international mechanical engineering congress and exposition. Vol. 86687, American Society of Mechanical Engineers; 2022, V006T08A068. http://dx.doi.org/10.1115/imece2022-94502.

[121] Hong Y-P, Lee D-Y, Choi Y-H, Hong S-K, Kim S-E. An experimental study on the extreme motion responses of a spar platform in the heave resonant waves. In: Proceedings of the fifteenth international offshore and polar engineering conference. Seoul, Korea. 2005, ISOPE–I–05–033.

[122] Ringwood JV, Davidson J, Giorgi S. Chapter 7 - identifying models using recorded data. In: Folley M, editor. Numerical modelling of wave energy converters. Academic Press; 2016, p. 123–47. http://dx.doi.org/10.1016/B978-0-12-803210-7.00007-4.

[123] Giorgi G, Davidson J, Habib G, Bracco G, Mattiazzo G, Kalmár-Nagy T. Nonlinear dynamic and kinematic model of a Spar-Buoy: Parametric resonance and yaw numerical instability. J Mar Sci Eng 2020;8(7):504. http://dx.doi.org/10.3390/jmse8070504.

[124] Folley M, Whittaker T. Spectral modelling of wave energy converters. Coast Eng 2010;57(10):892–7. http://dx.doi.org/10.1016/j.coastaleng.2010.05.007.

[125] Fujiyama ES, Lelkes J, Kalmár-Nagy T, Davidson J. A computationally efficient analytical modelling approach for parametric oscillations in floating bodies. 2024, http://dx.doi.org/10.21203/rs.3.rs-4014118/v1, Preprint.

[126] Giorgi G, Ringwood JV. Computationally efficient nonlinear Froude–Krylov force calculations for heaving axisymmetric wave energy point absorbers. J Ocean Eng Mar Energy 2017;3(1):21–33. http://dx.doi.org/10.1007/s40722-016-0066-2.

[127] Morison JR, Johnson JW, Schaaf SA, et al. The force exerted by surface waves on piles. J Pet Technol 1950;2(05):149–54. http://dx.doi.org/10.2118/950149-g.

[128] Giorgi G, Ringwood JV. Articulating parametric resonance for an OWC spar buoy in regular and irregular waves. J Ocean Eng Mar Energy 2018;4(4):311–22. http://dx.doi.org/10.1007/s40722-018-0124-z.

[129] Giorgi G, Gomes RPF, Bracco G, Mattiazzo G. Numerical investigation of parametric resonance due to hydrodynamic coupling in a realistic wave energy converter. Nonlinear Dynam 2020;101(1):1–18. http://dx.doi.org/10.1007/s11071-020-05739-8.

[130] Davidson J, Ringwood JV. Mathematical modelling of mooring systems for wave energy converters - a review. Energies 2017;10(5):666. http://dx.doi.org/10.3390/en10050666.

[131] Moideen H, Falzarano J. A critical assessment of ship parametric roll analysis. In: Proc. 11th int. ship stability workshop (ISSW), Wageningen, the Netherlands. 2010, p. 21–3.

[132] Buckham BJ. Dynamics modelling of low-tension tethers for submerged remotely operated vehicles (Ph.D. thesis), University of Victoria; 2003.

[133] Giorgi G, Gomes RPF, Henriques JCC, Gato LMC, Bracco G, Mattiazzo G. Detecting parametric resonance in a floating oscillating water column device for wave energy conversion: Numerical simulations and validation with physical model tests. Appl Energy 2020;276:115421. http://dx.doi.org/10.1016/j.apenergy.2020.115421.

[134] Bento N, Fontes M. Emergence of floating offshore wind energy: Technology and industry. Renew Sustain Energy Rev 2019;99:66–82. http://dx.doi.org/10.1016/j.rser.2018.09.035.

[135] Edwards EC, Holcombe A, Brown S, Ransley E, Hann M, Greaves D. Evolution of floating offshore wind platforms: A review of at-sea devices. Renew Sustain Energy Rev 2023;183:113416. http://dx.doi.org/10.1016/j.rser.2023.113416.

[136] Hamed YS, Aly AA, Saleh B, Alogla AF, Aljuaid AM, Alharthi MM. Nonlinear structural control analysis of an offshore wind turbine tower system. Processes 2019;8(1):22. http://dx.doi.org/10.3390/pr8010022.

[137] Abhinav KA, Saha N. Nonlinear dynamical behaviour of jacket supported offshore wind turbines in loose sand. Mar Struct 2018;57:133–51. http://dx.doi.org/10.1016/j.marstruc.2017.10.002.

[138] Ikeda T, Harata Y, Miyazawa Y, Ishida Y. Parametric resonances of floating wind turbines blades under vertical wave excitation. In: The 14th international conference on vibration engineering and technology of machinery. Vol. 211, MATEC Web of Conferences; 2018, p. 18004. http://dx.doi.org/10.1051/matecconf/201821118004.

[139] Gunnoo H, Abcha N, Mouazé D, Ezersky A, García-Hermosa MI. Laboratory simulation of resonance amplification of the hydrodynamic fields in the vicinity of wind farm masts. In: Proceedings of the 1st international conference on renewable energies offshore, Lisbon. 2014, http://dx.doi.org/10.1201/b18973-113.

[140] Abe K, Utsunomiya T. Study on parametric excitation of a spar platform. J Struct Constr Eng 2012;68(2):I813–22. http://dx.doi.org/10.2208/jscejam.68.I_813.

[141] Ma C, Iijima K, Fujikubo M. 2015A-GS4-4 control of subharmonic motion in tethered buoy system. In: Conference proceedings the Japan society of naval architects and ocean engineers 21. The Japan Society of Naval Architects and Ocean Engineers; 2015, p. 281–5.

[142] Ma C, Iijima K, Nihei Y, Fujikubo M. Theoretical, experimental and numerical investigations into nonlinear motion of a tethered-buoy system. J Mar Sci Technol 2016;21(3):396–415. http://dx.doi.org/10.1007/s00773-015-0362-x.

[143] Andersen T, Rasmus S, Nielsen K. Hydrodynamic excitation forces on floating structures with finite displacements. In: International ocean and polar engineering conference. ISOPE; 2015, ISOPE–I–15–819.

[144] Choi E-Y, Jeong W-B, Cho J-R. Combination resonances in forced vibration of spar-type floating substructure with nonlinear coupled system in heave and pitch motion. Int J Nav Archit Ocean Eng 2016;8(3):252–61. http://dx.doi.org/10.1016/j.ijnaoe.2016.03.004.

[145] Choi E-Y, Cho J-R, Jeong W-B. Numerical study on the resonance response of spar-type floating platform in 2-D surface wave. Struct Eng Mech 2017;63(1):37–46. http://dx.doi.org/10.12989/sem.2017.63.1.037.

[146] Wan L, Greco M, Lugni C, Gao Z, Moan T. A combined wind and wave energy-converter concept in survival mode: Numerical and experimental study in regular waves with a focus on water entry and exit. Appl Ocean Res 2017;63:200–16. http://dx.doi.org/10.1016/j.apor.2017.01.013.

[147] Li Y, Liu L, Zhu Q, Guo Y, Hu Z, Tang Y. Influence of vortex-induced loads on the motion of SPAR-type wind turbine: A coupled aero-hydro-vortex-mooring investigation. J Offshore Mech Arct Eng 2018;140(5):051903. http://dx.doi.org/10.1115/1.4040048.

[148] Vendrell L. Hydrostatic and hydrodynamic evaluation of a suction-stabilized float (Master's thesis), Arizona State University; 2013.

[149] Subramanian SC. Hydrodynamic study of a suction stabilized float (Master's thesis), Arizona State University; 2014.

[150] Susheelkumar CS, Redkar S, Sugar T. Parametric resonance and energy transfer in suction stabilized floating platforms: a brief survey. Int J Dyn Control 2017;5(3):931–45. http://dx.doi.org/10.1007/s40435-015-0210-1.

[151] Subramanian SC, Dye M, Redkar S. Dynamic analysis of suction stabilized floating platforms. J Mar Sci Eng 2020;8(8):587. http://dx.doi.org/10.3390/jmse8080587.

[152] Beraldo HDC, Franzini GR. A nonlinear mathematical model for dynamic analyses of a cantilevered beam with a tip-mass under support excitation. J Braz Soc Mech Sci Eng 2020;42(1):1–14. http://dx.doi.org/10.1007/s40430-019-2095-y.

[153] Aziminia MM, Abazari A, Behzad M, Hayatdavoodi M. Stability analysis of parametric resonance in spar-buoy based on floquet theory. Ocean Eng 2022;266:113090. http://dx.doi.org/10.1016/j.oceaneng.2022.113090.

[154] Ghozlane M, Najar F. Nonlinear analysis of a floating offshore wind turbine with internal resonances. Nonlinear Dynam 2023;112(3):1–29. http://dx.doi.org/10.1007/s11071-023-09120-3.

[155] Wei H, Xiao L, Tian X, Low YM. Nonlinear coupling and instability of heave, roll and pitch motions of semi-submersibles with bracings. J Fluids Struct 2018;83:171–93. http://dx.doi.org/10.1016/j.jfluidstructs.2018.09.002.

[156] Yu L, Li C, Wang S. Model tests and numerical simulations on the parametric resonance of the deep draft semi-submersible under regular waves. Ocean Eng 2022;243:110273. http://dx.doi.org/10.1016/j.oceaneng.2021.110273.

[157] Nishihara S, Imakita A. Parametric excitation in tension leg platform. J Soc Nav Archit Jpn 1979;1979(145):219–26. http://dx.doi.org/10.2534/jjasnaoe1968.1979.219.

[158] Rivera LA, Neves MAS, Cruz RE, Esperança PDTT. A study on unstable motions of a tension leg platform in close proximity to a large FPSO. In: Contemporary ideas on ship stability: risk of capsizing. Springer; 2019, p. 307–21. http://dx.doi.org/10.1007/978-3-030-00516-0_18.

[159] Shen W, Tan Z, Hu C. Sensitivity study on influencing factors of coupled motion characteristics for truss spar. IOP Conf Ser: Earth Environ Sci 2021;632(2):022054. http://dx.doi.org/10.1088/1755-1315/632/2/022054.

[160] Jose A, Falzarano J, Wang H. A study of negative damping in floating wind turbines using coupled program FAST-SIMDYN. In: International conference on offshore mechanics and arctic engineering. Vol. 51975, American Society of Mechanical Engineers; 2018, V001T01A036. http://dx.doi.org/10.1115/iowtc2018-1112.

[161] Jose A, Falzarano J. Jump bifurcation phenomenon during varying wind speeds in floating offshore wind turbines. J Offshore Mech Arct Eng 2022;144(3):034501. http://dx.doi.org/10.1115/1.4053541.

[162] Jonkman J. Influence of control on the pitch damping of a floating wind turbine. In: 46th AIAA aerospace sciences meeting and exhibit. 2008, p. 1306. http://dx.doi.org/10.2514/6.2008-1306.

[163] Christiansen S, Bak T, Knudsen T. Damping wind and wave loads on a floating wind turbine. Energies 2013;6(8):4097–116. http://dx.doi.org/10.3390/en6084097.

[164] Magar KT, Balas MJ. Adaptive individual blade pitch control to reduce platform pitch motion of a floating offshore wind turbine: preliminary study. In: Smart materials, adaptive structures and intelligent systems. Vol. 46148, American Society of Mechanical Engineers; 2014, V001T03A016. http://dx.doi.org/10.1115/smasis2014-7520.

[165] Olondriz J, Elorza I, Calleja C, Jugo J, Pujana A. Platform negative damping, blade root and tower base bending moment reductions with an advanced control technique. In: Proceedings of the windEurope conference and exhibition, Amsterdam, Netherlands. 2017.

[166] Jia Y. Review of nonlinear vibration energy harvesting: Duffing, bistability, parametric, stochastic and others. J Intell Mater Syst Struct 2020;31(7):921–44. http://dx.doi.org/10.1177/1045389x20905989.

[167] Rugar D, Grütter P. Mechanical parametric amplification and thermomechanical noise squeezing. Phys Rev Lett 1991;67(6):699. http://dx.doi.org/10.1103/physrevlett.67.699.

[168] Carr DW, Evoy S, Sekaric L, Craighead HG, Parpia JM. Parametric amplification in a torsional microresonator. Appl Phys Lett 2000;77(10):1545–7. http://dx.doi.org/10.1063/1.1308270.

[169] Jia Y, Seshia AA. An auto-parametrically excited vibration energy harvester. Sens Actuators A: Phys 2014;220:69–75. http://dx.doi.org/10.1016/j.sna.2014.09.012.

[170] Jia Y, Yan J, Soga K, Seshia AA. Parametric resonance for vibration energy harvesting with design techniques to passively reduce the initiation threshold amplitude. Smart Mater Struct 2014;23(6):065011. http://dx.doi.org/10.1088/0964-1726/23/6/065011.

[171] Yang W, Towfighian S. A parametric resonator with low threshold excitation for vibration energy harvesting. J Sound Vib 2019;446:129–43. http://dx.doi.org/10.1016/j.jsv.2019.01.038.

[172] Ding W, Song B, Mao Z, Wang K. Experimental investigations on a low frequency horizontal pendulum ocean kinetic energy harvester for underwater mooring platforms. J Mar Sci Technol 2016;21(2):359–67. http://dx.doi.org/10.1007/s00773-015-0357-7.

[173] Ding W, Mao Z, Cao H, Wang K. Performance evaluation of a two-directional energy harvester with low-frequency vibration. Smart Mater Struct 2020;29(5):055006. http://dx.doi.org/10.1088/1361-665x/ab7944.

[174] Franzini GR, Santos RCS, Pesce CP. A numerical study on piezoelectric energy harvesting by combining transverse galloping and parametric instability phenomena. J Mar Sci Appl 2017;16(4):465–72. http://dx.doi.org/10.1007/s11804-017-1439-1.

[175] Dern J-C. Unstable motion of free spar buoys in waves. In: Proceedings of the 9th symposium on naval hydrodynamics. 1972.

[176] Jingrui Z, Yougang T, Wenjun S. A study on the combination resonance response of a classic spar platform. J Vib Control 2010;16(14):2083–107. http://dx.doi.org/10.1177/1077546309349393.

[177] Sang S, Zhou Y, Jiang XL. Study on nonlinear motion behavior of coupled heave-pitch for the classic spar platform based on AQWA. Appl Mech Mater 2012;170:2170–4. http://dx.doi.org/10.4028/www.scientific.net/amm.170-173.2170.

[178] Gavassoni E, Gonçalves PB, Roehl DM. Nonlinear vibration modes and instability of a conceptual model of a spar platform. Nonlinear Dynam 2014;76(1):809–26. http://dx.doi.org/10.1007/s11071-013-1171-6.

[179] Liu L, Zhou B, Tang Y. Study on the nonlinear dynamical behavior of deepsea spar platform by numerical simulation and model experiment. J Vib Control 2014;20(10):1528–37. http://dx.doi.org/10.1177/1077546312472917.

[180] Li W, gang Tang Y, qin Liu L, Li Y, Wang B. Internal resonances for heave, roll and pitch modes of a spar platform considering wave and vortex-induced loads in the main roll resonance. China Ocean Eng 2017;31(4):408–17. http://dx.doi.org/10.1007/s13344-017-0047-9.

[181] Li W, Tang Y, Wang B, Li Y. Internal resonances for the heave roll and pitch modes of a spar platform considering wave and vortex exciting loads in heave main resonance. J Mar Sci Appl 2018;17(2):265–72. http://dx.doi.org/10.1007/s11804-018-0023-7.
[182] Li W, Tang Y, Liu L, Liu S, Cai R. Heave-roll-pitch coupled nonlinear internal resonance response of a spar platform considering wave and vortex exciting loads. J Ocean Univ China 2017;16(2):209–22. http://dx.doi.org/10.1007/s11802-017-3151-9.
[183] Rodríguez CA, Neves MAS. Investigation on parametrically excited motions of spar platforms in waves. In: Contemporary ideas on ship stability. Springer; 2019, p. 291–305. http://dx.doi.org/10.1007/978-3-030-00516-0_17.
[184] Habib G, Giorgi G, Davidson J. Coexisting attractors in floating body dynamics undergoing parametric resonance. Acta Mech 2022;233(6):2351–67. http://dx.doi.org/10.1007/s00707-022-03225-3.
[185] Davidson J, Kalmár-Nagy T, Habib G. Parametric excitation suppression in a floating cylinder via dynamic vibration absorbers: a comparative analysis. Nonlinear Dynam 2022;110(2):1081–108. http://dx.doi.org/10.1007/s11071-022-07710-1.
[186] Koo BJ, Kim MH, Randall RE. Mathieu instability of a spar platform with mooring and risers. Ocean Eng 2004;31(17–18):2175–208. http://dx.doi.org/10.1016/j.oceaneng.2004.04.005.
[187] Yan H. Computations of fully nonlinear three-dimensional wave-body interactions (Ph.D. thesis), Massachusetts Institute of Technology; 2010.
[188] Li B-B, Ou J-P, Teng B. Numerical investigation of damping effects on coupled heave and pitch motion of an innovative deep draft multi-spar. J Mar Sci Technol 2011;19(2):231–44. http://dx.doi.org/10.51400/2709-6998.2158.
[189] Huang L, Liu L, Liu C, Tang Y. The nonlinear bifurcation and chaos of coupled heave and pitch motions of a truss spar platform. J Ocean Univ China 2015;14(5):795–802. http://dx.doi.org/10.1007/s11802-015-2592-2.
[190] Neves MAS, Sphaier SH, Mattoso BM, Rodríguez CA, Santos AL, Vileti VL, Torres FGS. On the occurrence of mathieu instabilities of vertical cylinders. In: 27th international conference on offshore mechanics and arctic engineering. American Society of Mechanical Engineers; 2008, p. 619–27. http://dx.doi.org/10.1115/OMAE2008-57567.
[191] Rodríguez CA, Neves MAS. Nonlinear instabilities of spar platforms in waves. In: 31st international conference on ocean, offshore and arctic engineerering. American Society of Mechanical Engineers; 2012, p. 605–14. http://dx.doi.org/10.1115/omae2012-83577.
[192] Liu S, Tang Y, Li W. Nonlinear random motion analysis of coupled heave-pitch motions of a spar platform considering 1st-order and 2nd-order wave loads. J Mar Sci Appl 2016;15(2):166–74. http://dx.doi.org/10.1007/s11804-016-1349-7.
[193] Nallayarasu S, Mathai TP. Effect of mathieu instability on motion response of spar hull with heave damping plate. Ships Offshore Struct 2016;11(8):833–46. http://dx.doi.org/10.1080/17445302.2015.1073866.
[194] Yang H, Xu P. Effect of hull geometry on parametric resonances of spar in irregular waves. Ocean Eng 2015;99:14–22. http://dx.doi.org/10.1016/j.oceaneng.2015.03.006.
[195] Yang H, Xu P. Parametric resonance analyses for spar platform in irregular waves. China Ocean Eng 2018;32(2):236–44. http://dx.doi.org/10.1007/s13344-018-0025-x.
[196] Shen W, Tang Y. Stochastic analysis of nonlinear coupled heave-pitch motion for the truss spar platform. J Mar Sci Appl 2011;10(4):471–7. http://dx.doi.org/10.1007/s11804-011-1093-y.
[197] Francescutto A. An experimental investigation of parametric rolling in head waves. J Offshore Mech Arct Eng 2001;123(2):65–9. http://dx.doi.org/10.1115/1.1355247.
[198] Shin YS, Belenky VL, Paulling JR, Weems KM, Lin WM. Criteria for parametric roll of large containeships in longitudinal seas. Trans- Soc Nav Archit Mar Eng 2004;112(4):1153–71.
[199] Bulian G, Francescutto A, Lugni C. On the nonlinear modelling of parametric rolling in regular and irregular waves. Int ShipBuilding Prog 2004;51:173–203. http://dx.doi.org/10.3233/SHP-2004-51.2_3_5.
[200] Francescutto A, Bulian G. Nonlinear and stochastic aspects of parametric rolling modelling. Mar Technol SNAME News 2004;41(2):74–81.
[201] Bulian G. Nonlinear parametric rolling in regular waves - a general procedure for the analytical approximation of the GZ curve and its use in the time domain simulations. Ocean Eng 2005;32(3–4):309–30. http://dx.doi.org/10.1016/j.oceaneng.2004.08.008.
[202] Jensen JJ, Pedersen PT. Critical wave episodes for the assessment of parametric roll. In: Proceedings of the 9th international marine design conference. 2006.
[203] Jensen JJ. Efficient estimation of extreme non-linear roll motions using the first-order reliability method (FORM). J Mar Sci Technol 2007;12(4):191–202. http://dx.doi.org/10.1007/s00773-007-0243-z.
[204] Paulling JR, Rosenberg RM. On unstable ship motions resulting from nonlinear coupling. J Ship Res 1959;3(1):36–46. http://dx.doi.org/10.5957/jsr.1959.3.2.36.
[205] Oh IG, Nayfeh AH, Mook DT. Theoretical and experimental study of the nonlinearly coupled heave, pitch, and roll motions of a ship in longitudinal waves. In: Proceedings of the 14th biennial conference on mechanical vibration and noise. 1993, p. 105–25. http://dx.doi.org/10.1115/detc1993-0037.
[206] Oh IG, Nayfeh AH, Mook DT. A theoretical and experimental investigation of indirectly excited roll motion in ships. Philos Trans: Math Phys Eng Sci 2000;358(1771):1853–81. http://dx.doi.org/10.1098/rsta.2000.0618.
[207] Neves MAS, Perez NA, Valerio L. Stability of small fishing vessels in longitudinal waves. Ocean Eng 1999;26(12):1389–419. http://dx.doi.org/10.1016/s0029-8018(98)00023-7.
[208] Neves MAS, Rodriguez CA. A coupled third order model of roll parametric resonance. In: Guedes Soares C, Garbatov Y, Fonseca N, editors. Maritime transportation and exploitation of ocean and coastal resources. Taylor & Francis; 2005, p. 243–53. http://dx.doi.org/10.1201/9781439833728.ch29.
[209] France WN, Levadou M, Treakle TW, Paulling JR, Michel RK, Moore C. An investigation of head-sea parametric rolling and its influence on container lashing systems. Mar Technol SNAME News 2003;40(01):1–19. http://dx.doi.org/10.5957/mt1.2003.40.1.1.
[210] Belenky VL, Weems KM, Lin W-M, Paulling JR. Probabilistic analysis of roll parametric resonance in head seas. In: Almeida Santos Neves M, Belenky VL, de Kat JO, Spyrou K, Umeda N, editors. Contemporary ideas on ship stability and capsizing in waves. Dordrecht: Springer Netherlands; 2011, p. 555–69. http://dx.doi.org/10.1007/978-94-007-1482-3_31.
[211] Bulian G, Francescutto A, Umeda N, Hashimoto H. Qualitative and quantitative characteristics of parametric ship rolling in random waves in the light of physical model experiments. Ocean Eng 2008;35(17):1661–75. http://dx.doi.org/10.1016/j.oceaneng.2008.09.002.
[212] Levadou M, Palazzi L, Belenky V. Assessment of operational risks of parametric roll. Discussion. authors' closure. Trans- Soc Nav Archit Mar Eng 2003;111:517–34, The Society of Naval Architects and Marine Engineers: Papers Presented at the 2003 Annual Meeting.
[213] Holden C, Perez T, Fossen TI. Frequency-motivated observer design for the prediction of parametric roll resonance. IFAC Proc Vol 2007;40(17):57–62. http://dx.doi.org/10.3182/20070919-3-hr-3904.00011, 7th IFAC Conference on Control Applications in Marine Systems.
[214] McCue LS, Bulian G. A numerical feasibility study of a parametric roll advance warning system. J Offshore Mech Arct Eng 2007;129(3):165–75. http://dx.doi.org/10.1115/1.2746399.
[215] Galeazzi R, Perez T. A nonlinear observer for estimating transverse stability parameters of marine surface vessels. IFAC Proc Vol 2011;44(1):2967–71. http://dx.doi.org/10.3182/20110828-6-it-1002.01474, 18th IFAC World Congress.
[216] Yu L, Ma N, Gu X. Early detection of parametric roll by application of the incremental real-time Hilbert–Huang transform. Ocean Eng 2016;113:224–36. http://dx.doi.org/10.1016/j.oceaneng.2015.12.050.
[217] Acanfora M, Krata P, Montewka J, Kujala P. Towards a method for detecting large roll motions suitable for oceangoing ships. Appl Ocean Res 2018;79:49–61. http://dx.doi.org/10.1016/j.apor.2018.07.005.
[218] Acanfora M, Balsamo F. The smart detection of ship severe roll motions and decision-making for evasive actions. J Mar Sci Eng 2020;8(6):415. http://dx.doi.org/10.3390/jmse8060415.
[219] Luthy V, Grinnaert F, Billard J-Y, Rapp J. Real-time identification of parametric roll. J Ship Res 2023;67(03):174–83. http://dx.doi.org/10.5957/josr.07220021.
[220] Galeazzi R, Blanke M, Poulsen NK. Parametric roll resonance detection on ships from nonlinear energy flow indicator. IFAC Proc Vol 2009;42(8):348–53. http://dx.doi.org/10.3182/20090630-4-ES-2003.00058, 7th IFAC Symposium on Fault Detection, Supervision and Safety of Technical Processes.
[221] Galeazzi R, Blanke M, Poulsen NK. Parametric roll resonance detection using phase correlation and log-likelihood testing techniques. IFAC Proc Vol 2009;42(18):316–21. http://dx.doi.org/10.3182/20090916-3-br-3001.0037.
[222] Galeazzi R, Blanke M, Poulsen NK. Early detection of parametric roll resonance on container ships. IEEE Trans Control Syst Technol 2012;21(2):489–503. http://dx.doi.org/10.1109/tcst.2012.2189399.
[223] Galeazzi R, Blanke M, Falkenberg T, Poulsen NK, Violaris N, Storhaug G, Huss M. Parametric roll resonance monitoring using signal-based detection. Ocean Eng 2015;109:355–71. http://dx.doi.org/10.1016/j.oceaneng.2015.08.037.
[224] Míguez González M, López Peña F, Díaz Casás V, Galeazzi R, Blanke M. Prediction of parametric roll resonance by multilayer perceptron neural network. In: 21st international offshore and polar engineering conference. 2011, ISOPE–I–11–565.
[225] González MM, Casás VD, Peña FL, Rojas LP. Experimental parametric roll resonance characterization of a stern trawler in head seas. In: Proceedings of the 11th international conference on the stability of ships and ocean vehicles. 2012, p. 1–11.
[226] González MM, Casás VD, Peña FL, Rojas LP. On the application of artificial neural networks for the real time prediction of parametric roll resonance. In: Contemporary ideas on ship stability: from dynamics to criteria. Springer; 2023, p. 335–49. http://dx.doi.org/10.1007/978-3-031-16329-6_20.
[227] Zhou X, Li H, Huang Y, Liu Y. Deep learning machine based ship parametric rolling simulation and recognition algorithms. Ocean Eng 2023;276:114137. http://dx.doi.org/10.1016/j.oceaneng.2023.114137.
[228] Li X, Ma N, Shi Q, Gu X. Real-time prediction of parametric roll motion based on power-activation feed-forward neural network using measured data from model experiments. In: International ocean and polar engineering conference. ISOPE; 2023, ISOPE–I–23–338.

[229] Galeazzi R, Vidic-Perunovic J, Blanke M, Jensen JJ. Stability analysis of the parametric roll resonance under non-constant ship speed. In: Engineering systems design and analysis. Vol. 48364, 2008, p. 743–50. http://dx.doi.org/10.1115/esda2008-59453.

[230] Breu D, Fossen TI. Extremum seeking speed and heading control applied to parametric roll resonance. IFAC Proc Vol 2010;43(20):28–33. http://dx.doi.org/10.3182/20100915-3-de-3008.00003.

[231] Breu DA, Fossen TI. $\mathcal{L}_1$ adaptive and extremum seeking control applied to roll parametric resonance in ships. In: 2011 9th IEEE international conference on control and automation. ICCA, IEEE; 2011, p. 871–6. http://dx.doi.org/10.1109/ICCA.2011.6138047.

[232] Breu DA, Feng L, Fossen TI. Optimal speed and heading control for stabilization of parametric oscillations in ships. Parametr Reson Dyn Syst 2012;213–38. http://dx.doi.org/10.1007/978-1-4614-1043-0_11.

[233] Holden C, Breu DA, Fossen TI. Frequency detuning control by Doppler shift. Parametr Reson Dyn Syst 2012;193–212. http://dx.doi.org/10.1007/978-1-4614-1043-0_10.

[234] Umeda N, Hashimoto H, Minegaki S, Matsuda A. An investigation of different methods for the prevention of parametric rolling. J Mar Sci Technol 2008;13(1):16–23. http://dx.doi.org/10.1007/s00773-007-0253-x.

[235] Galeazzi R, Blanke M. On the feasibility of stabilizing parametric roll with active bifurcation control. IFAC Proc Vol 2007;40(17):50–6. http://dx.doi.org/10.3182/20070919-3-hr-3904.00010.

[236] Holden C, Galeazzi R, Perez T, Fossen TI. Stabilization of parametric roll resonance with active U-tanks via Lyapunov control design. In: Proceedings of the 10th European control conference. 2009, p. 4889–94. http://dx.doi.org/10.23919/ECC.2009.7075174.

[237] Galeazzi R, Holden C, Blanke M, Fossen TI. Stabilization of parametric roll resonance by combined speed and fin stabilizer control. In: Proceedings of the 10th European control conference. 2009, p. 4895–900. http://dx.doi.org/10.23919/ECC.2009.7075175.

[238] Holden C, Fossen TI. A U-tank control system for ships in parametric roll resonance. In: Parametric resonance in dynamical systems. Springer; 2011, p. 239–63. http://dx.doi.org/10.1007/978-1-4614-1043-0_12.

[239] Söder C-J, Rosén A, Ovegård E, Kuttenkeuler J, Huss M. Parametric roll mitigation using rudder control. J Mar Sci Technol 2013;18(3):395–403. http://dx.doi.org/10.1007/s00773-013-0216-3.

[240] Yu L, Taguchi K, Kenta A, Ma N, Hirakawa Y. Model experiments on the early detection and rudder stabilization of KCS parametric roll in head waves. J Mar Sci Technol 2018;23(1):141–63. http://dx.doi.org/10.1007/s00773-017-0463-9.

[241] Witz JA. Parametric excitation of crane loads in moderate sea states. Ocean Eng 1995;22(4):411–20. http://dx.doi.org/10.1016/0029-8018(94)00015-y.

[242] Kang H-S, Tang CH-H, Quen LK, Steven A, Yu X. Parametric resonance avoidance of offshore crane cable in subsea lowering operation through A* heuristic planner. Indian J Geo Mar Sci 2017;46(12):2422–33.

[243] Chin C-M, Nayfeh AH, Mook DT. Dynamics and control of ship-mounted cranes. J Vib Control 2001;7(6):891–904. http://dx.doi.org/10.1177/107754630100700607.

[244] Vázquez C, Collado J, Fridman L. Control of a parametrically excited crane: A vector Lyapunov approach. IEEE Trans Control Syst Technol 2013;21(6):2332–40. http://dx.doi.org/10.1109/tcst.2012.2233739.

[245] Vazquez C, Collado J, Fridman L. Super twisting control of a parametrically excited overhead crane. J Franklin Inst 2014;351(4):2283–98. http://dx.doi.org/10.1016/j.jfranklin.2013.02.011.

[246] Rainey RCT. Dynamics of tethered platforms. In: The royal institution of naval architects, spring meetings. 1977, Vol. Paper No. 6.

[247] Radhakrishnan S, Datla R, Hires RI. Theoretical and experimental analysis of tethered buoy instability in gravity waves. Ocean Eng 2007;34(2):261–74. http://dx.doi.org/10.1016/j.oceaneng.2006.01.010.

[248] Shah AA, Umar A, Siddiqui NA. A methodology for assessing the reliability of taut and slack mooring systems against instability. Ocean Eng 2005;32(10):1216–34. http://dx.doi.org/10.1016/j.oceaneng.2004.11.002.

[249] Cantero D, Rønnquist A, Naess A. Recent studies of parametrically excited mooring cables for submerged floating tunnels. Procedia Eng 2016;166:99–106. http://dx.doi.org/10.1016/j.proeng.2016.11.571.

[250] Cantero D, Rønnquist A, Naess A. Tension during parametric excitation in submerged vertical taut tethers. Appl Ocean Res 2017;65:279–89. http://dx.doi.org/10.1016/j.apor.2017.05.002.

[251] Lopes GJV. Contributions to the investigation of the nonlinear dynamics of immersed slender structures: reduced-order model analysis and their advantages (Ph.D. thesis), Universidade de São Paulo; 2022, http://dx.doi.org/10.11606/t.3.2022.tde-25112022-083551.

[252] Hara K, Shimojima K, Yamaguchi T. Development of an efficient calculation technique for dynamics of mooring lines by using discrete forms of rotation. J Fluids Struct 2023;122:103962. http://dx.doi.org/10.1016/j.jfluidstructs.2023.103962.

[253] Strickland GE, Mason AB. Parametric response of tlp tendons-theoretical and numerical analyses. In: Offshore technology conference. OTC; 1981, p. OTC–4071. http://dx.doi.org/10.4043/4071-MS.

[254] Patel MH, Park HI. Dynamics of tension leg platform tethers at low tension. Part I - mathieu stability at large parameters. Mar Struct 1991;4(3):257–73. http://dx.doi.org/10.1016/0951-8339(91)90004-u.

[255] Xiao F, Yang HZ. Probabilistic assessment of parametric instability of a top tensioned riser in irregular waves. J Mar Sci Technol 2014;19(3):245–56. http://dx.doi.org/10.1007/s00773-013-0243-0.

[256] Li L, Chen L. Parametric instability analysis of the top-tensioned riser in consideration of complex pre-stress distribution. Adv Mech Eng 2018;10(1):1687814017753894. http://dx.doi.org/10.1177/1687814017753894.

[257] Franzini GR, Mazzilli CEN. Non-linear reduced-order model for parametric excitation analysis of an immersed vertical slender rod. Int J Non-Linear Mech 2016;80:29–39. http://dx.doi.org/10.1016/j.ijnonlinmec.2015.09.019.

[258] Yang H, Xiao F, Xu P. Parametric instability prediction in a top-tensioned riser in irregular waves. Ocean Eng 2013;70:39–50. http://dx.doi.org/10.1016/j.oceaneng.2013.05.002.

[259] Yang H, Xiao F. Instability analyses of a top-tensioned riser under combined vortex and multi-frequency parametric excitations. Ocean Eng 2014;81:12–28. http://dx.doi.org/10.1016/j.oceaneng.2014.02.006.

[260] Wu Z, Xie C, Mei G, Dong H. Dynamic analysis of parametrically excited marine riser under simultaneous stochastic waves and vortex. Adv Struct Eng 2019;22(1):268–83. http://dx.doi.org/10.1177/1369433218783968.

[261] Yuan Y, Xue H, Tang W. VIV response characteristics of a top-tensioned riser with bi-frequency parametric excitation. Ocean Eng 2019;190:106490. http://dx.doi.org/10.1016/j.oceaneng.2019.106490.

[262] Kang HS. Semi-active magneto-rheological damper and applications in tension leg platform/semi-submersible (Ph.D. thesis), Texas A&M University; 2015.

[263] Franzini GR, Sato BS, Campedelli GR. Numerical analysis of a non-linear energy sink (NES) for the parametric excitation of a submerged cylinder. In: Proceedings of the 9th European nonlinear dynamics conference-ENOC2017. 2017.

[264] Jianjun Y, Tang S, Xiancheng W, Jiaqi W, Zhenshuai W, Chenguang X. Vibration analysis of the subsea dynamic umbilical under parametric excitations. In: INTER-NOISE and NOISE-CON congress and conference proceedings. no. 8, Institute of Noise Control Engineering; 2019, p. 1573–82.

[265] Gambaudo J-M. Perturbation of a Hopf bifurcation by an external time-periodic forcing. J Differential Equations 1985;57(2):172–99. http://dx.doi.org/10.1016/0022-0396(85)90076-2.

[266] Rand R, Barcilon A, Morrison T. Parametric resonance of Hopf bifurcation. Nonlinear Dynam 2005;39:411–21. http://dx.doi.org/10.1007/s11071-005-3400-0.

[267] Spyrou KJ. The stability of floating regular solids. Ocean Eng 2022;257:111615. http://dx.doi.org/10.1016/j.oceaneng.2022.111615.

[268] Sequeira D, Mann BP. Potential well hopping and performance of ocean energy harvesters. J Sound Vib 2020;465:115008. http://dx.doi.org/10.1016/j.jsv.2019.115008.

[269] Sequeira D, Little J, Mann BP. Investigating threshold escape behavior for the gimballed horizontal pendulum system. J Sound Vib 2019;450:47–60. http://dx.doi.org/10.1016/j.jsv.2019.03.008.

[270] Trahan R, Kalmár-Nagy T. Equilibrium, stability, and dynamics of rectangular liquid-filled vessels. J Comput Nonlinear Dyn 2011;6(4):041012. http://dx.doi.org/10.1115/1.4003915.

[271] Falzarano JM, Clague RE, Kota RS. Application of nonlinear normal mode analysis to the nonlinear and coupled dynamics of a floating offshore platform with damping. Nonlinear Dynam 2001;25:255–74. http://dx.doi.org/10.1007/978-94-017-2452-4_14.

[272] Gavassoni E, Gonçalves PB, Roehl DDM. Nonlinear vibration modes of an offshore articulated tower. Ocean Eng 2015;109:226–42. http://dx.doi.org/10.1016/j.oceaneng.2015.08.028.

[273] Meng S, Song S, Che C, Zhang W. Internal flow effect on the parametric instability of deepwater drilling risers. Ocean Eng 2018;149:305–12. http://dx.doi.org/10.1016/j.oceaneng.2017.12.031.

[274] Wang H, Falzarano J. Efficient assessment for the pitchpoling risks of a generic wave energy converter based on first passage statistics. Ocean Eng 2022;257:111619. http://dx.doi.org/10.1016/j.oceaneng.2022.111619.

[275] Wang H, Falzarano J. The pitch vulnerability of a typical wave energy converter geometry based on Melnikov and Markov approaches. Ships Offshore Struct 2021;16(8):904–18. http://dx.doi.org/10.1080/17445302.2020.1787932.

[276] Ding R, Zhang H, Xu D, Liu C, Shi Q, Liu J, Zou W, Wu Y. Experimental and numerical study on motion instability of modular floating structures. Nonlinear Dynam 2023;111(7):6239–59. http://dx.doi.org/10.1007/s11071-022-08163-2.

[277] Patel MS, Liew MS, Mustaffa Z, Yee NC, Whyte A. Development of downtime cost calculator for offloading operations influenced by parametric rolling. J Mar Sci Eng 2019;8(1):7. http://dx.doi.org/10.3390/jmse8010007.